

# Single-cell and Spatial isoform Transcriptomics

Kévin Lebrigand  
Computational Biology Core  
IPMC, CNRS, Côte d'Azur University, France

 lebrigand@ipmc.cnrs.fr  
 @kevinlebrigand



# Overview

---

## 01 - Single-cell transcriptomics

## 02 - Single-cell isoform transcriptomics (scNaUMI-seq)

Article | Open Access | Published: 12 August 2020

### High throughput error corrected Nanopore single cell transcriptome sequencing

Kevin Lebrigand , Virginie Magnone, Pascal Barbuy  & Rainer Waldmann 

*Nature Communications* 11, Article number: 4025 (2020) | [Cite this article](#)

## 03 - Spatial isoform transcriptomics (SiT)

### The spatial landscape of gene expression isoforms in tissue sections

Kevin Lebrigand, Joseph Bergenstråhlé, Kim Thrane, Annelie Mollbrink, Konstantinos Meletis, Pascal Barbuy , Rainer Waldmann, Joakim Lundeberg | Author Notes

*Nucleic Acids Research*, Volume 51, Issue 8, 8 May 2023, Page e47, <https://doi.org/10.1093/nar/gkad169>

Published: 17 March 2023 | [Article history](#) 

## 04 - Spatial single-cell imaging-based transcriptomics

# 01

## Single-cell transcriptomics

# Single-cell Transcriptomics

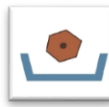
Context

---

Bulk mRNA libraries  
100ng total RNA  
(10,000 cells)



Single cell mRNA libraries  
10 pg total RNA  
(<<1pg mRNA)



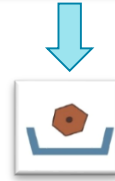
# Single-cell Transcriptomics

Unique Molecular Identifiers (UMI)

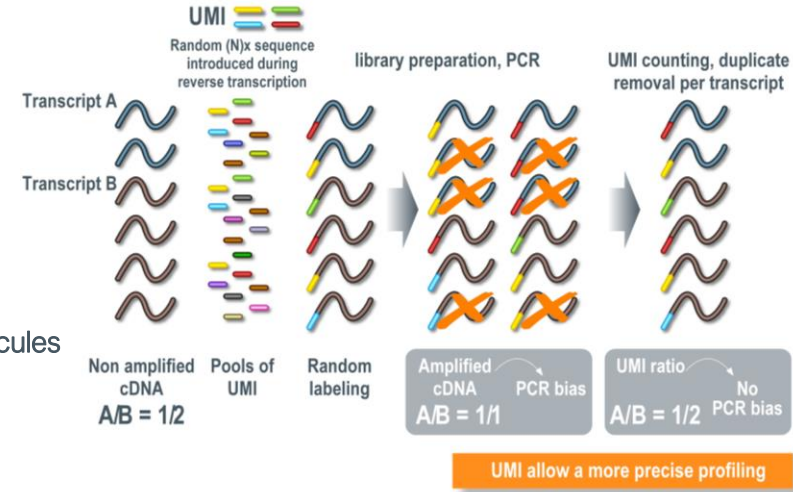
Bulk mRNA libraries  
100ng total RNA  
(10,000 cells)



Single cell mRNA libraries  
10 pg total RNA  
(<<1pg mRNA)

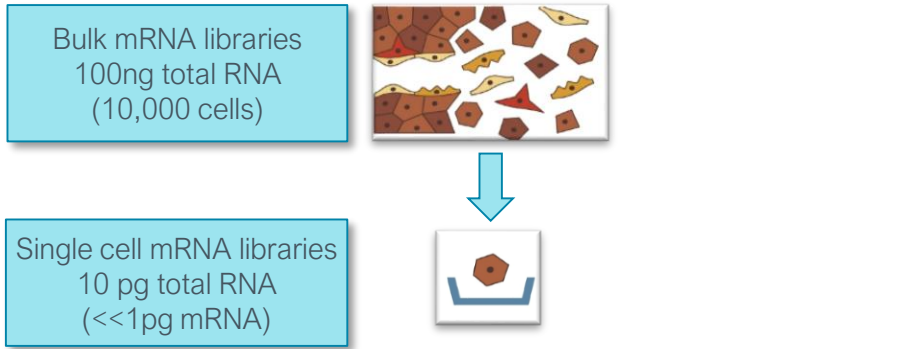


- Elimination of PCR amplification bias and artefacts
- Use of Unique Molecular Identifiers (UMI) to monitor the **number of molecules**
  - Kivioja, T. et al. Counting absolute numbers of molecules using unique molecular identifiers. Nat Meth 9, 72-74 (2012)
  - Improved accuracy of molecule counting



# Single-cell Transcriptomics

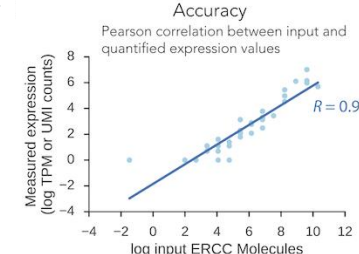
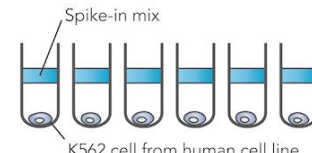
ERCC spike-in allow capture efficiency evaluation



- Elimination of PCR amplification bias and artefacts
- Highly efficient library preparation techniques
- Spike-in ERCC molecules allow yield and **capture efficiency** evaluation

ERCC (External RNA Controls Consortium)

- set of 92 RNA sequences,
- of varying length and GC content,
- mixed at known concentrations,
- 22 abundance levels that are spaced one fold change apart from each other



Power Analysis of Single Cell RNA-Sequencing Experiments, Svensson et al., 2018

# Single-cell Transcriptomics

How much RNA does a typical mammalian cell contain?

Bulk mRNA libraries  
100ng total RNA  
(10,000 cells)



Single cell mRNA libraries  
10 pg total RNA  
(<<1pg mRNA)

- Cell RNA content depend on its cell type and developmental stage
- Majority of RNA molecules are tRNAs and rRNAs, mRNA accounts for only 1-5%
- Approximately 360,000 mRNA molecules are present in a single mammalian cell
- ~ 12,000 different transcripts with a typical length of around 2 kb,
- Some comprise 3% of the mRNA pool whereas others account for less than 0.1%. These rare or low-abundance mRNAs may have a copy number of only 5-15 molecules per cell.

<https://www.qiagen.com/fr/resources/faq?id=06a192c2-e72d-42e8-9b40-3171e1eb4cb8&lang=en>

## Average total RNA yields

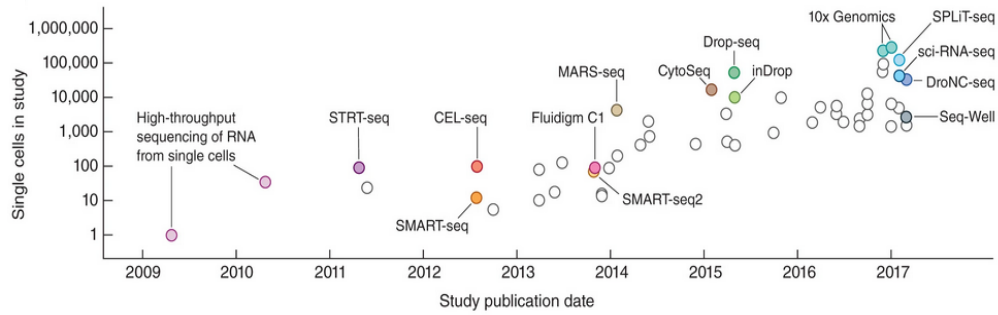
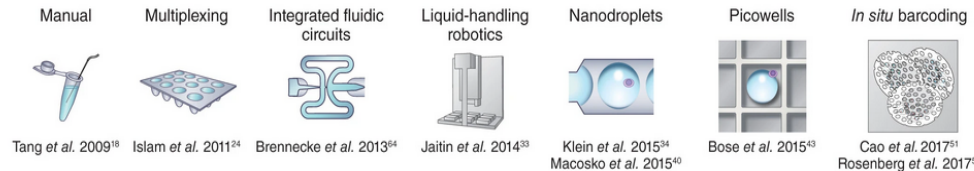
Cell lines ( $1 \times 10^6$ cells)	Total RNA (μg)
Dendritic cells, human	4
Hematopoietic progenitor cells (CD34 $^{+}$ ), human	1
Fibroblasts, rat	5
PBMC	8

## Cell lines ( $1 \times 10^6$ cells)

Cell lines ( $1 \times 10^6$ cells)	Total RNA (μg)
Colon carcinoma cells	30
HEK 293 cells	16
HeLa cells	32
HUV-EC-C	38
THP1 cells	16
U937 cells	12

# Single-cell transcriptomics

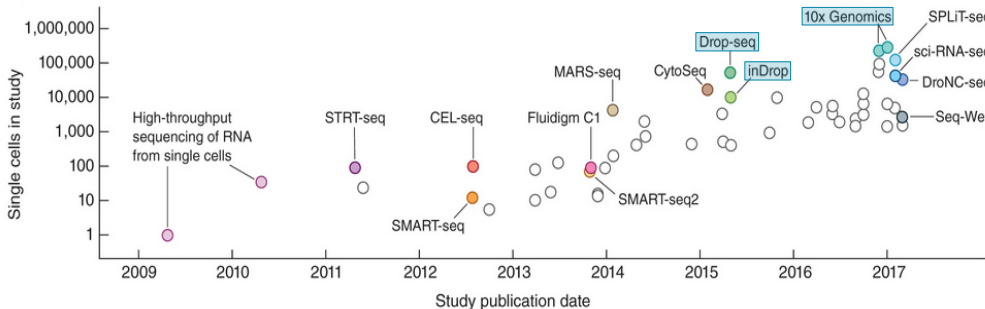
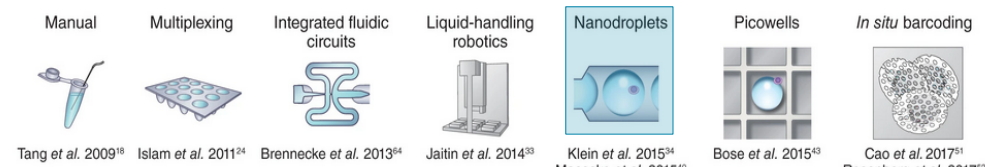
Evolution of isolation techniques and throughput



Exponential scaling of single-cell RNA-seq in the past decade  
Svensson *et al.*, *Nature Protocols*, 2018

# Single-cell transcriptomics

## Droplet-based approaches

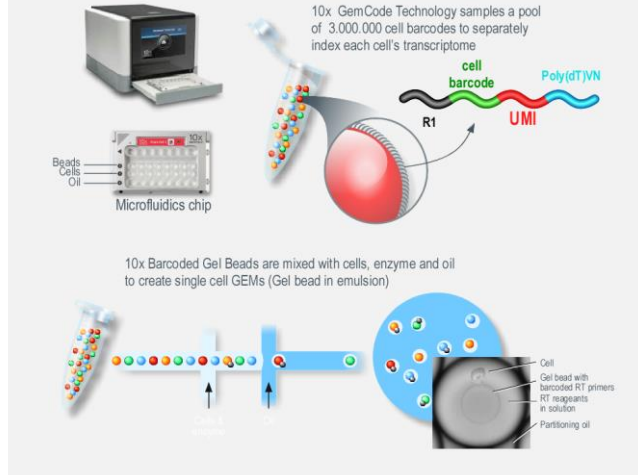


Exponential scaling of single-cell RNA-seq in the past decade  
Svensson et al., *Nature Protocols*, 2018

InDrop, Klein et al, 2015  
Drop-seq, Macosko et al, 2015  
10x Genomics, Zheng et al, 2016

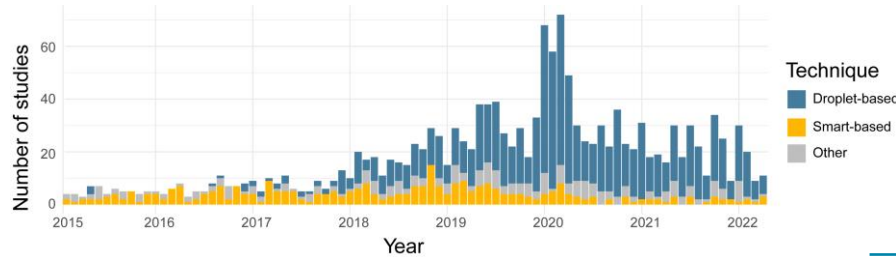
## 10x Genomics Chromium single cell controller (2016)

- Easy-to-set-up and robust workflow
- High scalability (1,3M cells dataset)



# Single-cell transcriptomics

Single cell approaches in publications



A curated database reveals trends in single cell transcriptomics  
Svensson et al., Database , 2020

- Huge amount of single-cell studies in the past 5 years,
- Droplet-based approaches = 61% (Chromium: 47%)

Technique	Count
Chromium	725
Smart-seq2	177
SMARTer (C1)	124
Drop-seq	74
SMARTer	28
InDrops	23
CITE-seq	18
CEL-seq2	17
STRT-seq	16
MARS-seq	16
Tang	15
CEL-seq	13
STRT-seq (C1)	13
Seq-Well	13
SORT-seq	12
BD Rhapsody	11
BioMark	8
GemCode	7
ICELL8	7
Perturb-seq	7
Patch-seq	6
sc-RT-mPCR	6
MERFISH	5

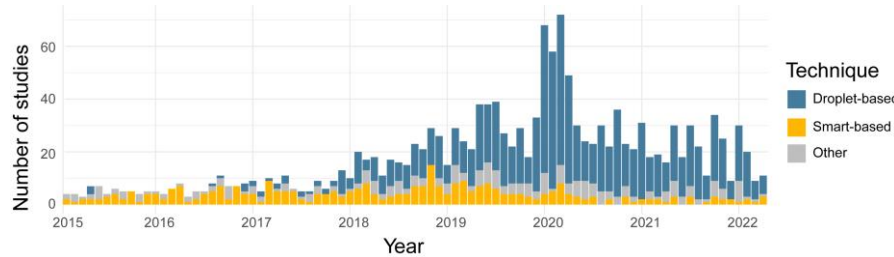
## Droplet-based approaches

- Digital Gene Expression (UMI)
- High cell number throughput
- Limited capture efficiency (<10%)
- 3p or 5p signal (SAGE-like)



# Single-cell transcriptomics

Single cell approaches in publications



A curated database reveals trends in single cell transcriptomics  
Svensson et al., Database , 2020

- Huge amount of single-cell studies in the past 5 years,
- Droplet-based approaches = 61% (Chromium: 47%)
- Smart-based approach = 21%, <5% in the last 2 years

Technique	Count
Chromium	725
Smart-seq2	177
SMARTer (C1)	124
Drop-seq	74
SMARTer	28
InDrops	23
CITE-seq	18
CEL-seq2	17
STRT-seq	17
MARS-seq	16
Tang	15
CEL-seq	13
STRT-seq (C1)	13
Seq-Well	13
SORT-seq	12
BD Rhapsody	11
BioMark	8
GemCode	7
ICELL8	7
Perturb-seq	7
Patch-seq	6
sc-RT-mPCR	6
MERFISH	5

## Smart-based approach

- Lower cell number (384-well plate handling)
- Higher capture efficiency (~30%)
- No UMI before v3 (May 2020)
- Full-length coverage using short-reads

Article | Open Access | Published: 30 May 2022

## Scalable single-cell RNA sequencing from full transcripts with Smart-seq3xpress

Michael Hagemann-Jensen, Christoph Ziegenhain & Rickard Sandberg

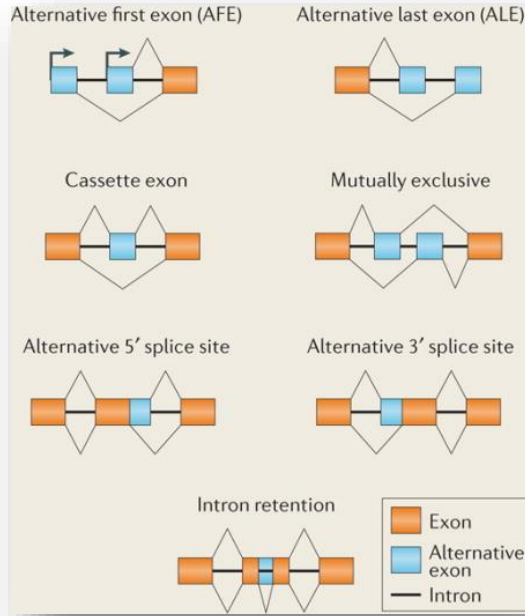
Brief Communication | Open Access | Published: 30 May 2022

## Fast and highly sensitive full-length single-cell RNA sequencing using FLASH-seq

Vincent Hahaut, Dinko Pavlinic, Walter Carbone, Sven Schuerer, Pierre Balmer, Mathieu Quinodoz, Magdalena Renner, Guglielmo Roma, Cameron S. Cowan & Simone Picelli

# Transcriptomics

Complex outcomes of alternative splicing



- 90% of the genes are subjected to alternative splicing,
- Gencode v42 : 252,416 distinct isoforms for 62,696 genes,
- On average, a human gene contains **8.8 exons**, mean size of 145 nt,
- Average encodes mRNA **2,410 nt** long :



Alternative splicing and disease  
Tazi et al., 2008

Scotti and Swanson, Nat Rev Genet., 2016

# 02

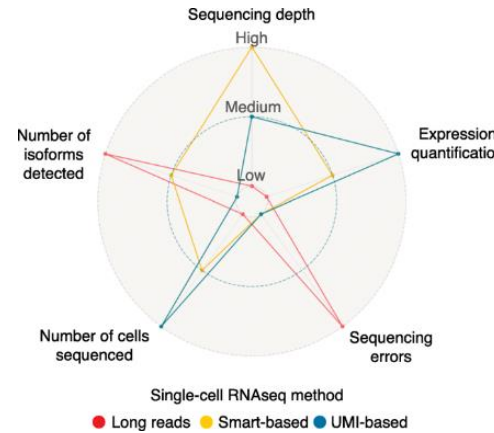
## Single-cell isoform transcriptomics

# Requirement for single-cell full-length transcriptomics

Arzalluz-Luque et al., 2018

Four required conditions :

- full-length transcript sequencing using long reads,
- low sequencing errors and artefacts,
- high number of cells sequenced,
- high capture efficiency and sequencing depth



Main approaches :

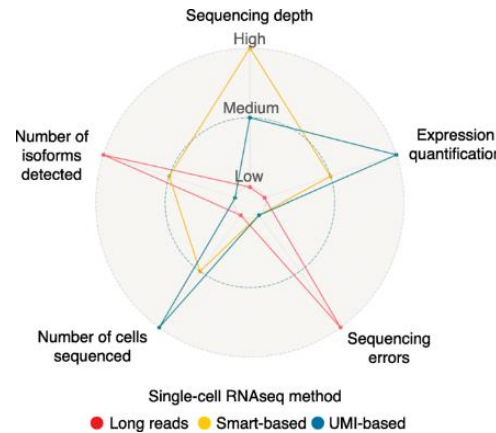
- **Smart-based** methods, produce short reads across the entire transcript length, cannot accommodate UMIs, short reads difficult to assign unambiguously to isoform.
- **UMI-based** methods, limited to sequencing of the 3' (or 5' end), well suited to accurate gene-level expression quantification.
- **Long-reads** (i.e. single molecule) allows a sequencing of each transcript molecule as a single read providing full isoform connectivity, but suffers from a high prevalence of sequencing errors.

# Requirement for single-cell full-length transcriptomics

Arzalluz-Luque et al., 2018

Four required conditions :

- full-length transcript sequencing using long reads,
- low sequencing errors and artefacts,
- high number of cells sequenced,
- high capture efficiency and sequencing depth



Main approaches :

- **Smart-based** methods, produce short reads across the entire transcript length, cannot accommodate UMIs, short reads difficult to assign unambiguously to isoform.
- **UMI-based** methods, limited to sequencing of the 3' (or 5' end), well suited to accurate gene-level expression quantification.
- **Long-reads** (i.e. single molecule) allows a sequencing of each transcript molecule as a single read providing full isoform connectivity, but suffers from a high prevalence of sequencing errors.



nature  
COMMUNICATIONS

Article | Open Access | Published: 12 August 2020

## High throughput error corrected Nanopore single cell transcriptome sequencing

Kevin Lebrigand , Virginie Magnone, Pascal Barbuy  & Rainer Waldmann 

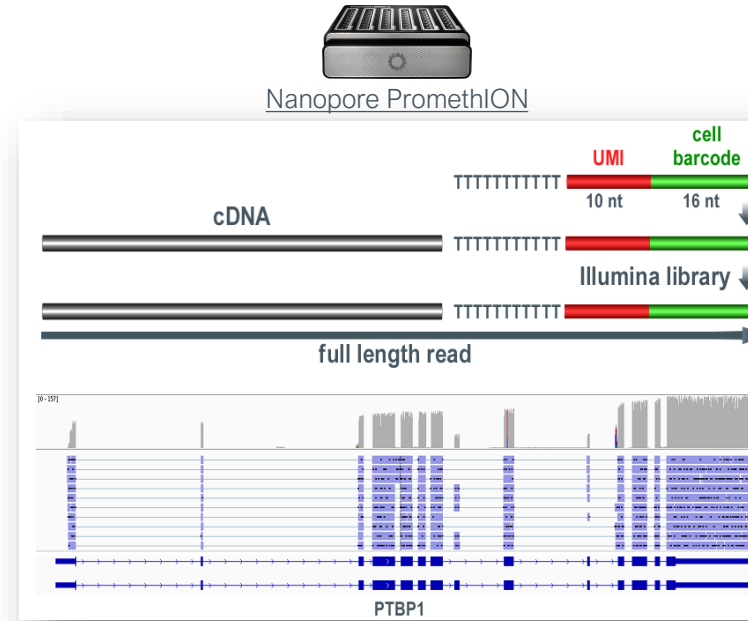
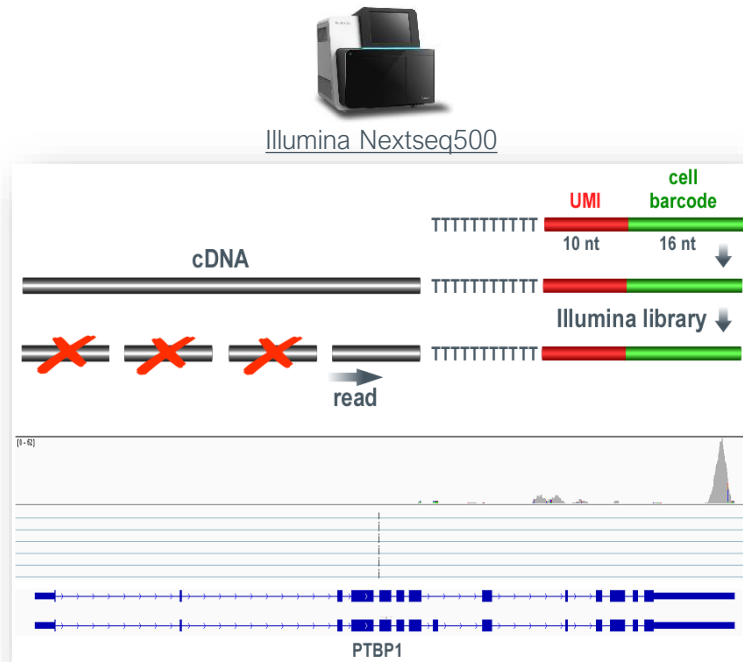
*Nature Communications* 11, Article number: 4025 (2020) | Cite this article

6251 Accesses | 61 Altmetric | Metrics

[scNaUMI-seq protocol](#)

# Single-cell long-read transcriptomics

Droplets-based approach short reads vs long reads



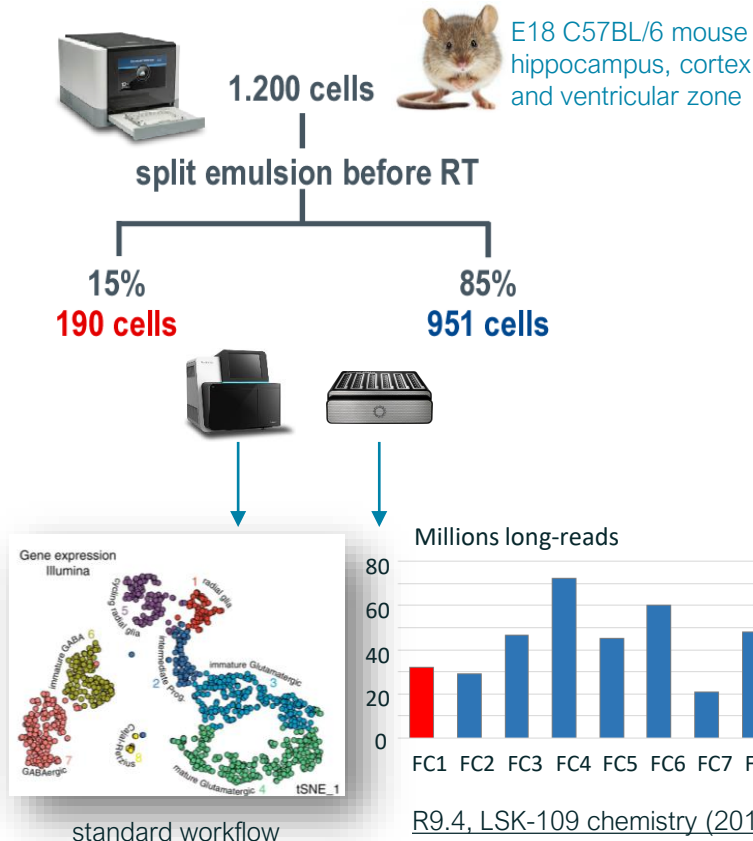
Information on alternative splicing, fusion transcripts, SNV, editing, imprinting

is lost

remain accessible

# Single-cell long-read transcriptomics

SiCeLoRe, bioinformatics for Single Cell Long Read



## nature communications

Explore content ▾ About the journal ▾ Publish with us ▾

nature > nature communications > articles > article

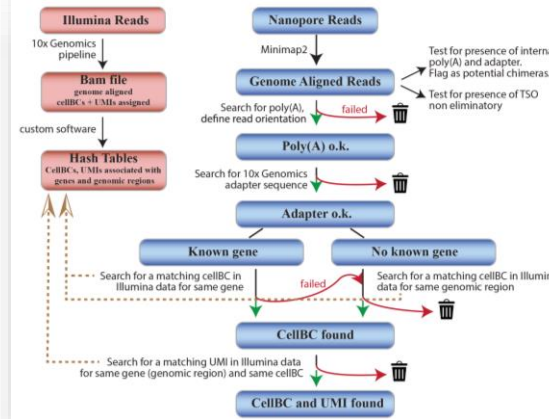
Article | Open Access | Published: 12 August 2020

### High throughput error corrected Nanopore single cell transcriptome sequencing

Kevin Lebrigand, Virginie Magnone, Pascal Barbuy & Rainer Waldmann

Nature Communications 11, Article number: 4025 (2020) | Cite this article

20k Accesses | 38 Citations | 58 Altmetric | Metrics



<https://github.com/ucagenomix/sicelore>

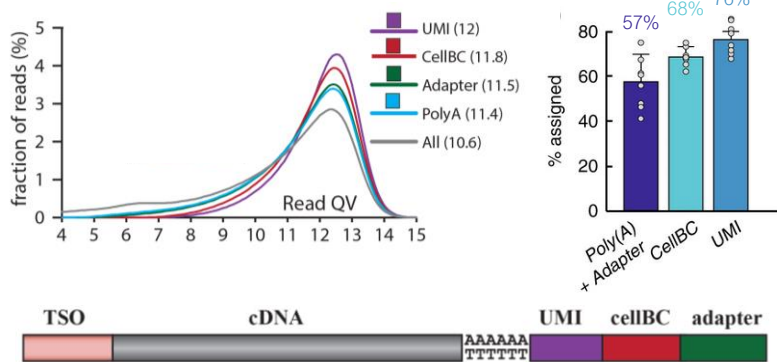


Rainer Waldmann

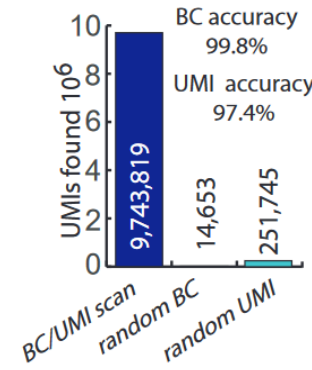
# Illumina-guided demultiplexing strategy

Barcodes assignment accuracy

Efficiency of cell barcode / UMI assignment



Accuracy of cell barcode / UMI assignment



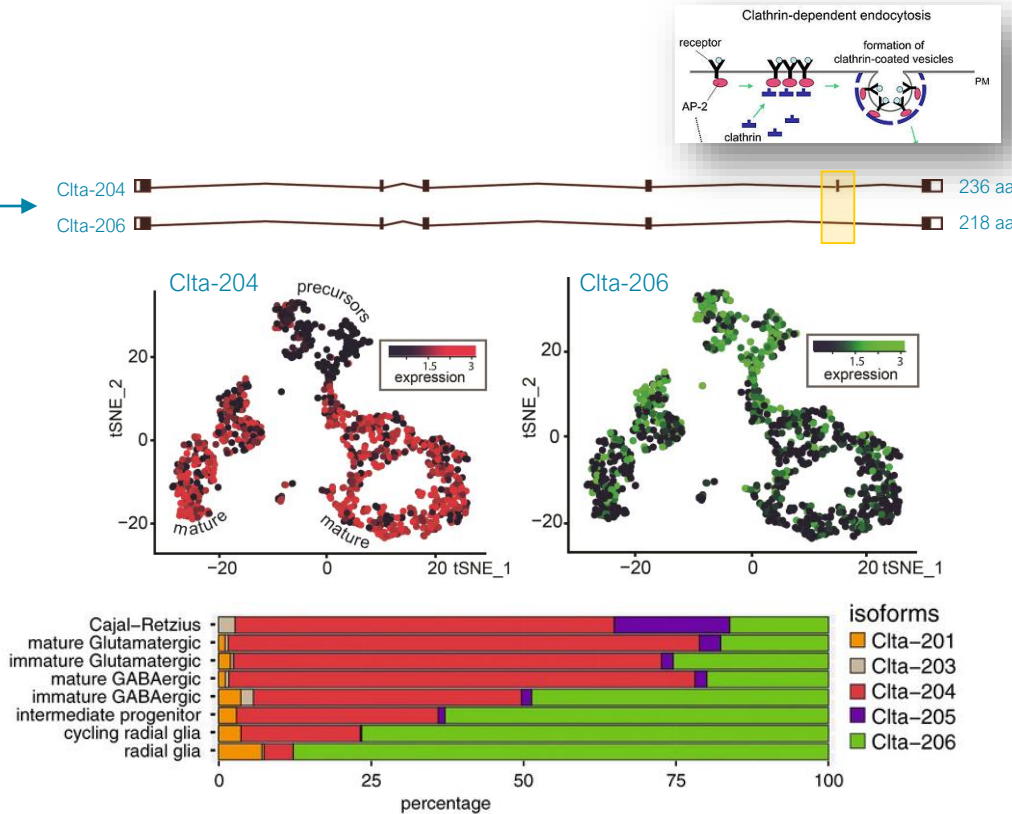
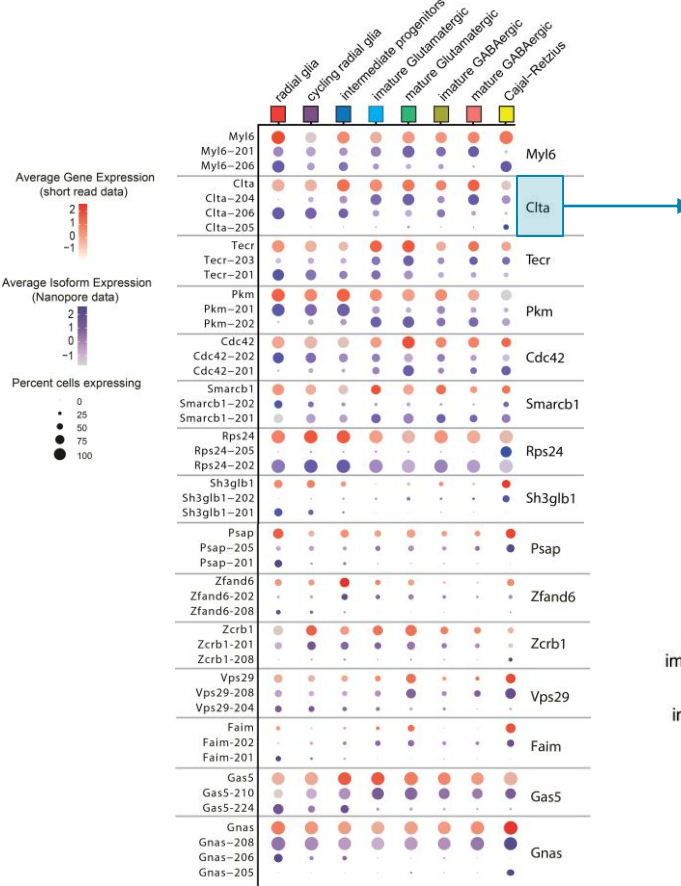
30% of the Nanopore reads were assigned to a cell barcode and UMI

## Reasons for losses

- Low QV reads
- PCR artefacts : TSO or poly(A) on both sides
- Out-of-cell barcodes (empty droplet RNA)
- UMI not in Illumina dataset (low sequencing saturation)

# Single-cell long-read transcriptomics reveals diversity

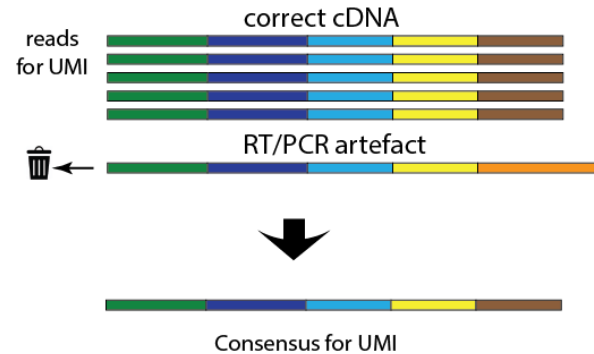
76 isoform-switching genes along neuronal maturation



# Single-cell long-read transcriptomics reveals sequence heterogeneity

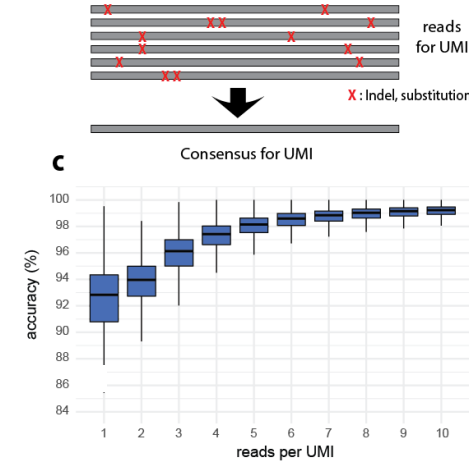
Consensus sequence computation per UMI

UMIs enable elimination of PCR artifacts



Crucial for accurate novel isoform discovery

UMIs enable correction of sequencing errors

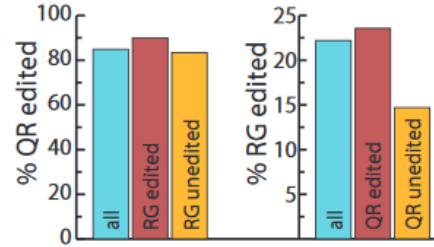
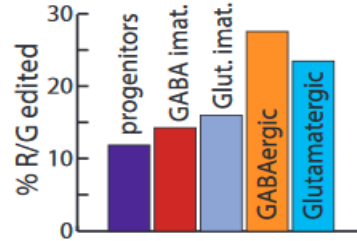
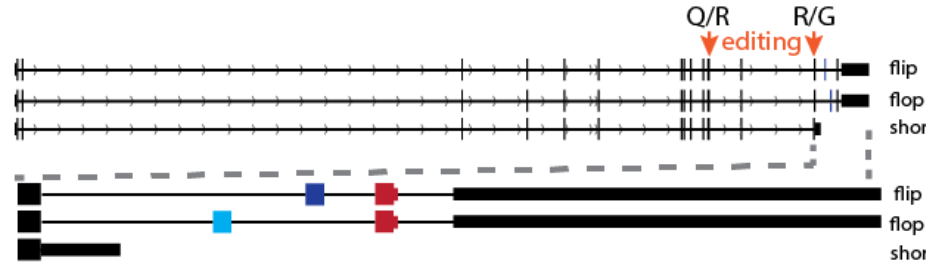
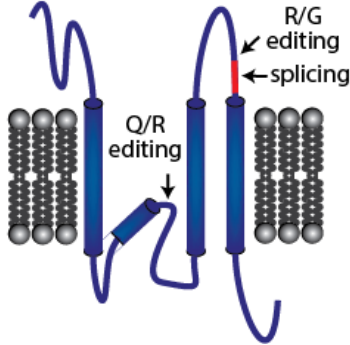


High accuracy for Single Nucleotide Variation call

# Long read sequencing reveals sequence heterogeneity

RNA A-to-I editing of the AMPA receptor Gria2

Q/R site regulates AMPA receptor  $\text{Ca}^{2+}$ -permeability  
R/G site is involved in desensitization and recovery of the receptor



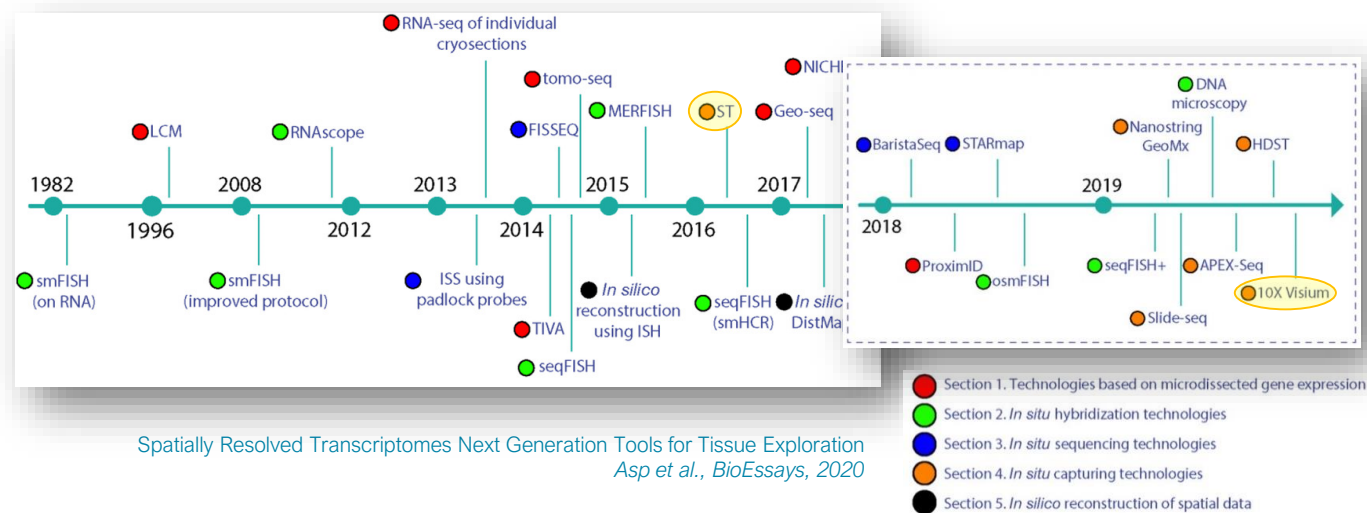
# 03

## Spatial isoform transcriptomics

# Spatial Transcriptomics approaches

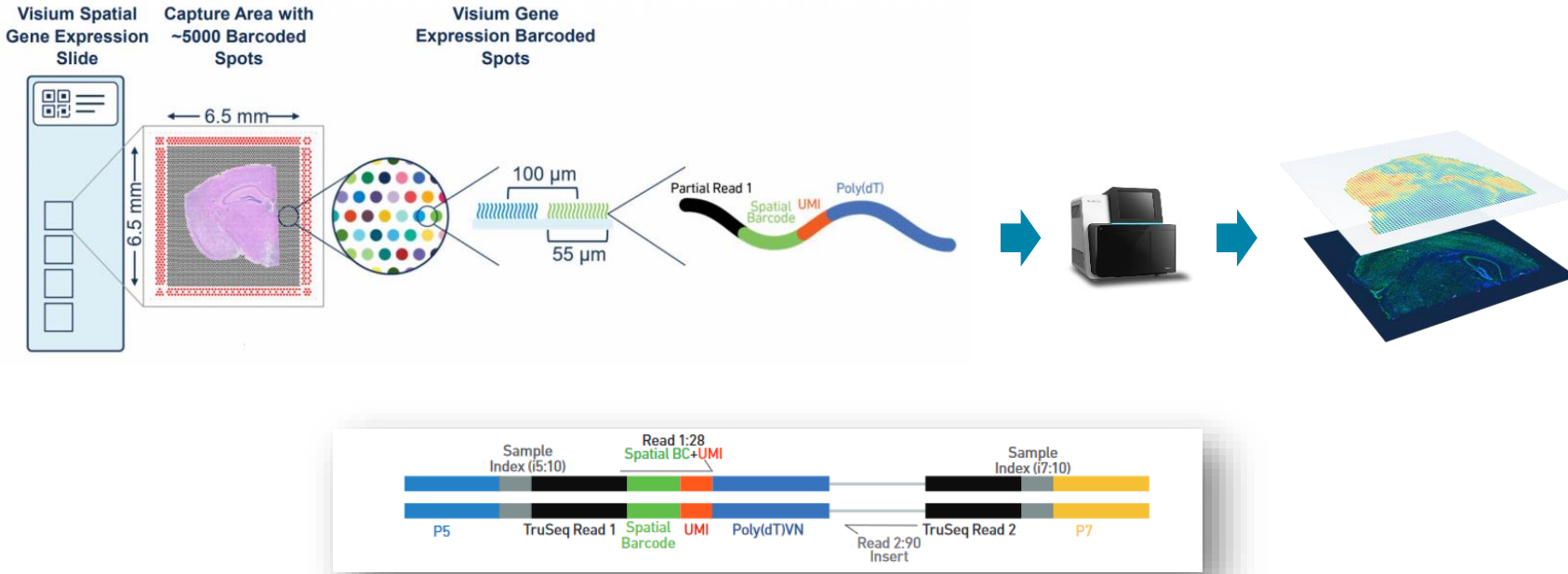
## Historical timeline

- Spatial transcriptomics aims at directly visualize gene expression in their original environment,
- It tackles the main limitation of single cell experiment missing the spatial organization,
- A lot of developments in the last years thanks to recent advances in different fields,



# In-situ capture spatial transcriptomics

10x Genomics Visium (2019)



→ Spatial barcode / UMI assignment strategy identical to single cell transcriptomics

# Spatial isoform Transcriptomics (SiT)

Nucleic Acids Research, 2023

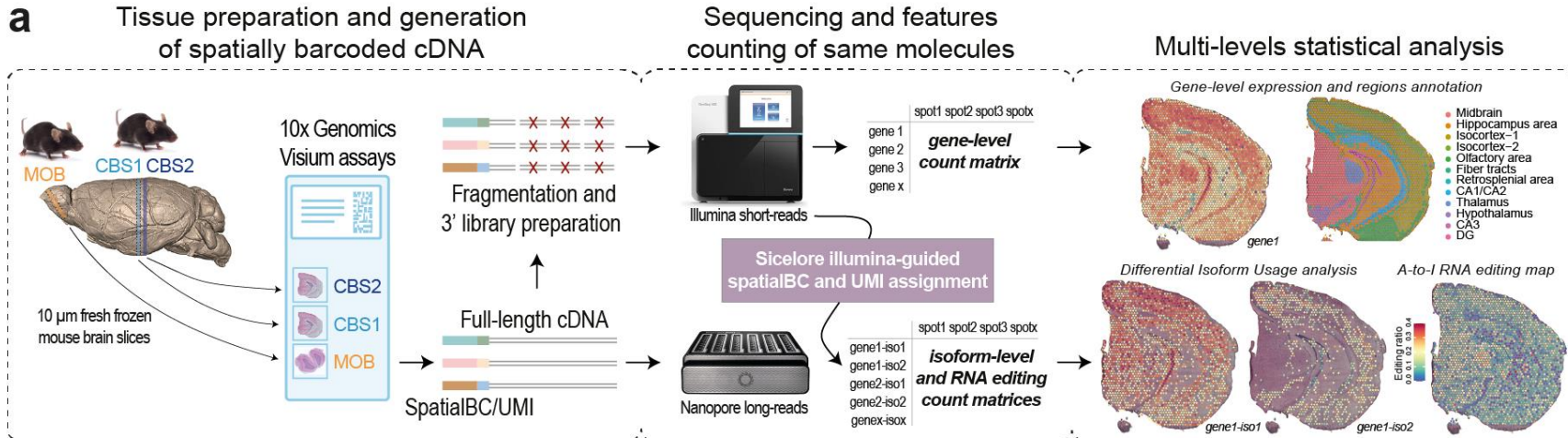
## The spatial landscape of gene expression isoforms in tissue sections

Kevin Lebrigand, Joseph Bergenstråle, Kim Thrane, Annelie Mollbrink, Konstantinos Meletis, Pascal Barbuy , Rainer Waldmann, Joakim Lundeberg Author Notes

Nucleic Acids Research, Volume 51, Issue 8, 8 May 2023, Page e47, <https://doi.org/10.1093/nar/gkad169>

Published: 17 March 2023 Article history ▾

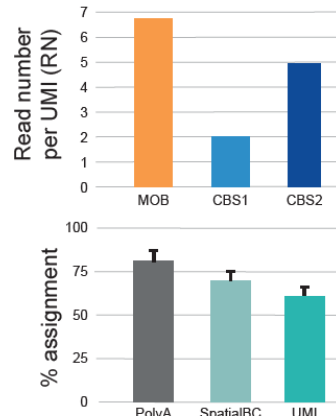
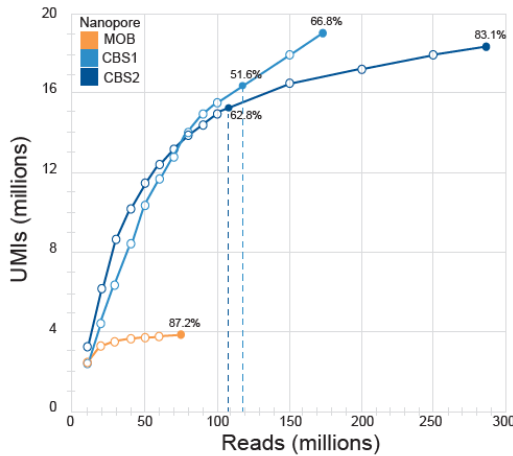
a



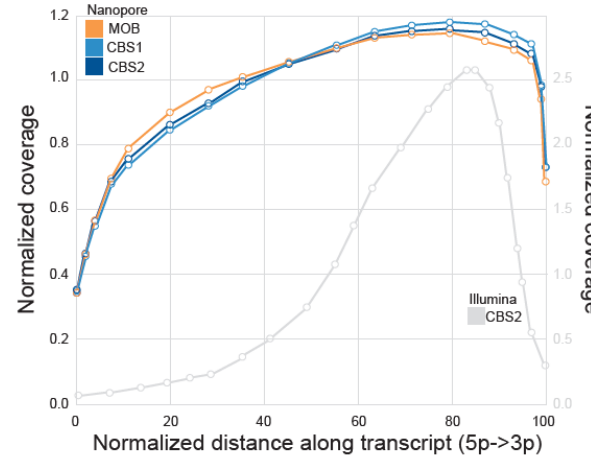
# Nanopore promethION long-read sequencing

Provides isoform-level spatial transcriptomics

## Sequencing saturation curves per samples



## Transcripts full-length coverage



Reads	MOB	
Date	18 feb. 20	20 mar. 20
Flow cells	PAE06474	PAE59649
Total reads (fastq_pass)	27628000	47272000
PolyA and Adapter found reads	21318117	47970311
SpatialBC found reads	14506264	29316718
UMIs found reads	10445006	19328468

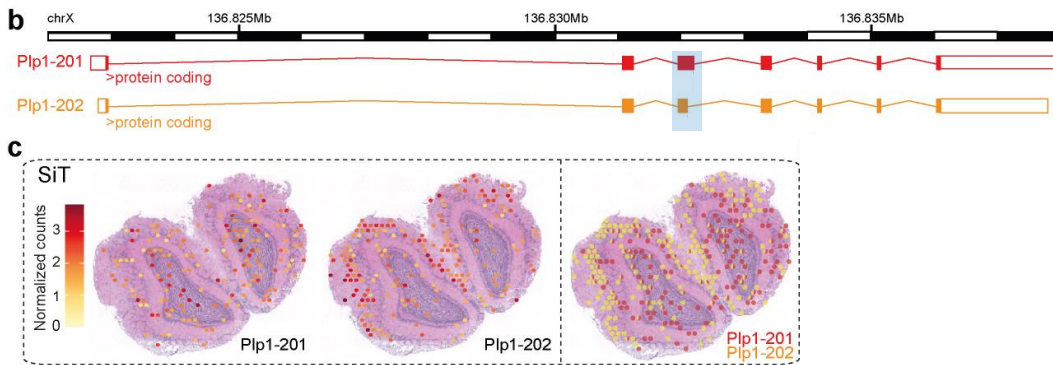
Reads	CBS1		
Date	18 feb. 20	20 mar. 20	24 feb. 21
Flow cells	PAE01745	PAE59645	PAG52067
Total reads (fastq_pass)	24980000	31736000	117280000
PolyA and Adapter found reads	17980183	27286678	80516212
SpatialBC found reads	12554655	19051597	54323311
UMIs found reads	7323748	10517081	27584331

Reads	CBS2								Total	%age
Date	12 may 20	13 may 20	19 may 20	25 may 20	25 may 20	26 may 20	27 may 20	09 feb. 21	Total	%age
Flow cells	PAE59606	PAE59231	PAE32756	PAE32753	PAE31188	PAE21339	PAD99555	PAG56368	13	
Total reads (fastq_pass)	22897702	30405384	27492770	18534938	31506774	19108718	25596387	110916000	535354673	
PolyA and Adapter found reads	18536047	25199992	22871198	16088962	26777546	15983663	21682530	85837208	428048647	79.96
SpatialBC found reads	14613934	19867830	14666481	11403706	19099469	11266930	14090779	60154119	294915793	68.90
UMIs found reads	8616415	11714126	7557944	12657620	7448718	9031708	34225619	175797856	59.61	of SpatialBC found reads

CBS1: One flow cell, 117 M reads → 51.6% sequencing saturation  
 CBS2: One flow cell, 111 M reads → 62.2% sequencing saturation  
 → 1 or 2 PromethION flow cells per slice

# SiT reveals specific splicing pattern across MOB regions

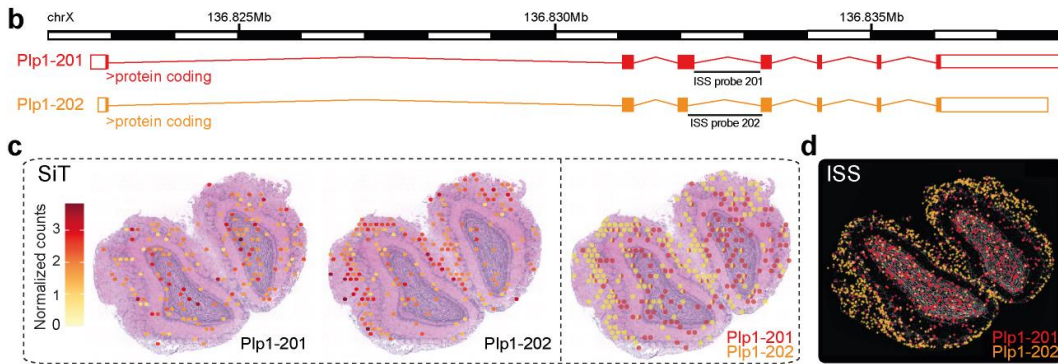
Plp1 Differential Transcript Usage (DTU)



Proteolipid Protein 1 (Plp1) is a gene involved in severe pathologies associated with CNS dysmyelination

# SiT reveals specific splicing pattern across MOB regions

Plp1 Differential Transcript Usage (DTU)



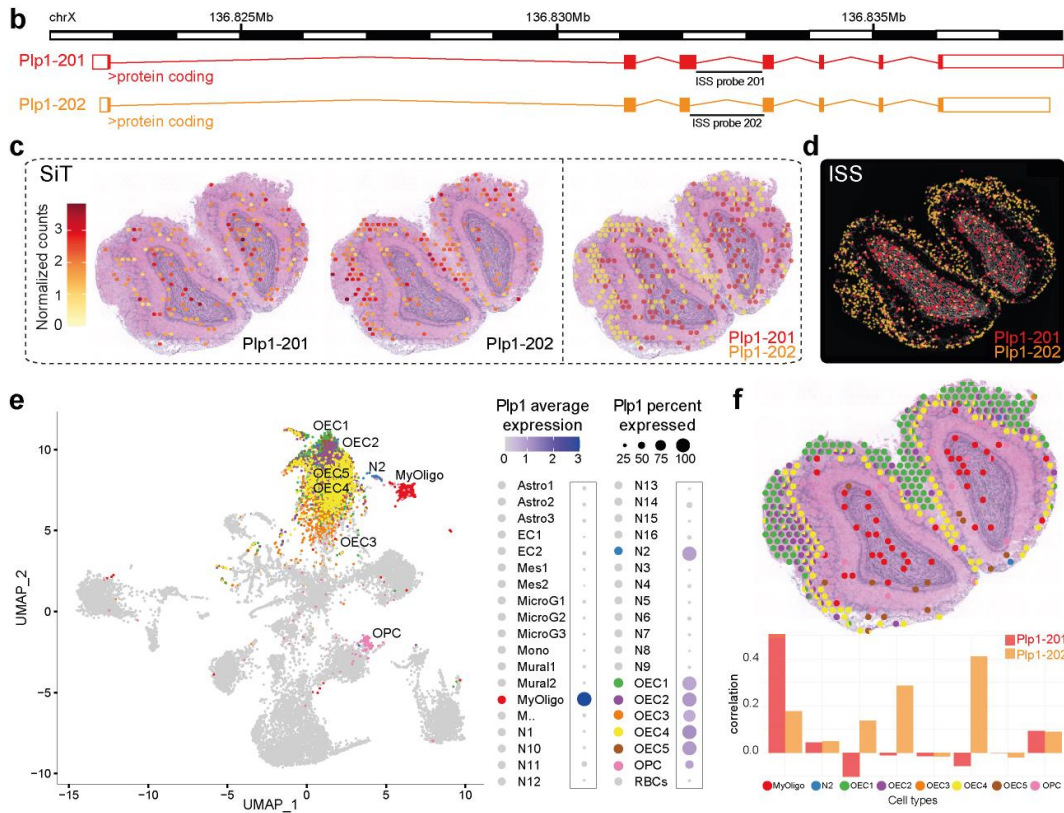
Proteolipid Protein 1 (Plp1) is a gene involved in severe pathologies associated with CNS dysmyelination



In Situ Sequencing Data

# SiT reveals specific splicing pattern across MOB regions

Cell type deconvolution using single cell external dataset (Tepe et al., 2018)

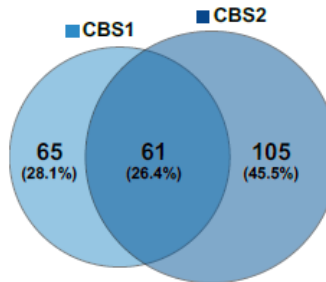
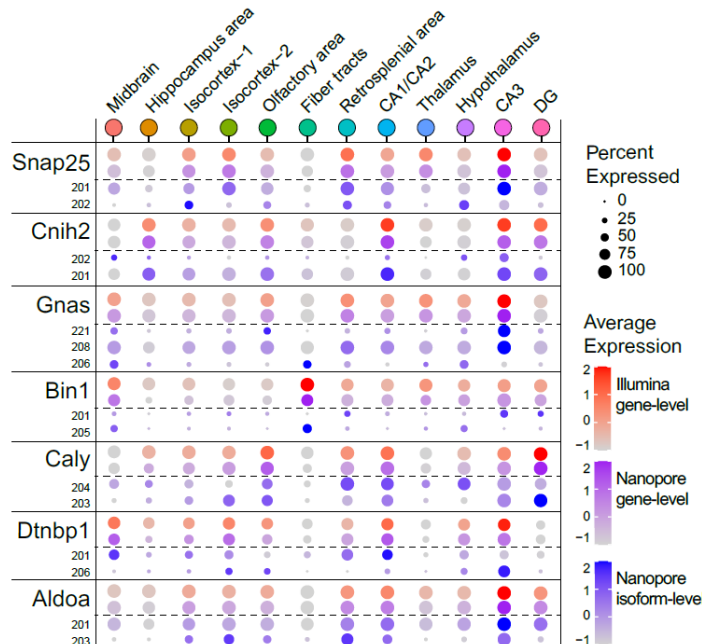


Proteolipid Protein 1 (Plp1) is a gene involved in severe pathologies associated with CNS dysmyelination

Spatial spot deconvolution of prominent *Plp1* expresser cell types. Correlation Deconvolution score / *Plp1* isoforms expression correlation shows that *Plp1* is predominantly expressed as *Plp1-202* by olfactory ensheathing cells (OEC) in the ONL and as *Plp1-201* isoform by myelinating-oligodendrocytes (MyOligo) in the GCL.

# Differential Transcript Usage (DTU) across CBS regions

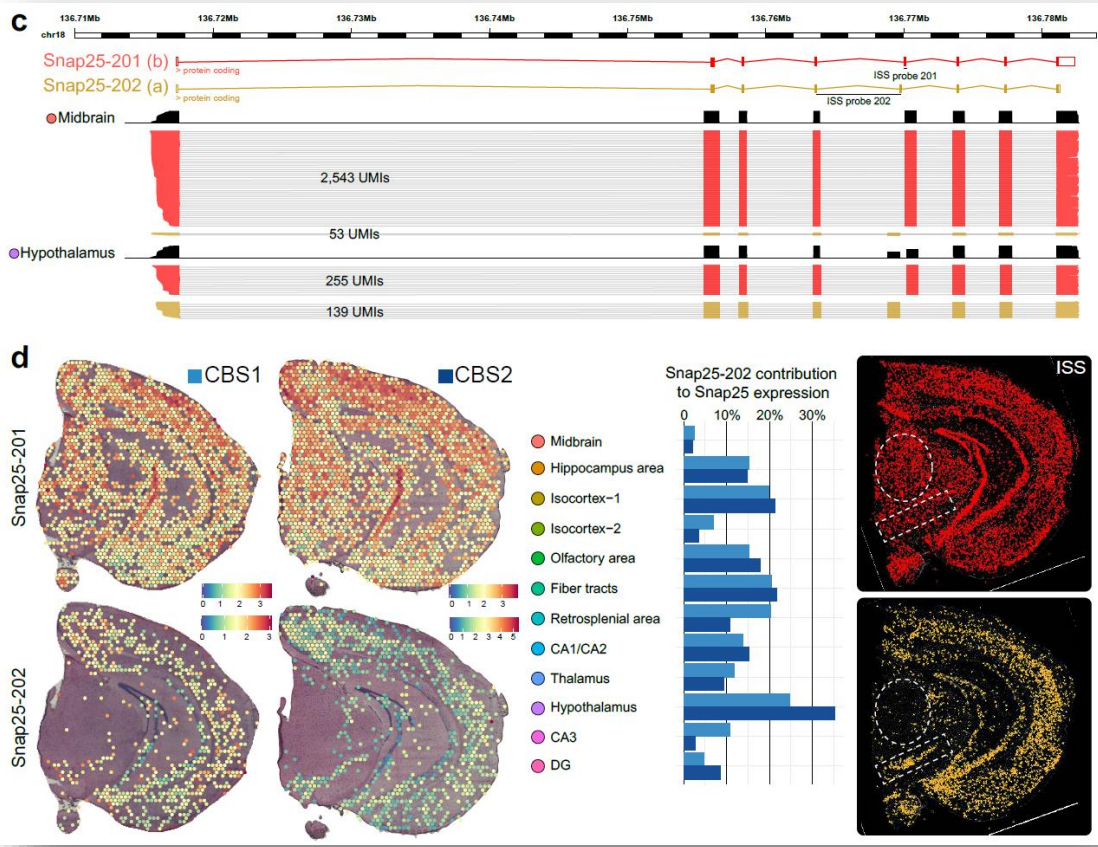
61 common switching genes detected



61 common switching genes in "CBS1" and "CBS2"						
Anapc11	Capzb	Eno2	Kctd13	Pcp4	Rpn1	
Ap2m1	Cck	Ensa	Kctd17	Pnkd	Rps24	
App	Cdc42	Faim	Mff	Polr2g	Rps6	
Arl2bp	Cltc	Fam173a	Mrpl48	Polr2h	S100a16	
Atp5g1	Cltb	Fis1	Mrpl55	Ppp1r1a	Sept8	
Bbip1	Cnih1	Fkbp8	Myl6	Ppp3ca	Sft2d1	
BC031181	Cspg5	Ftl1	Nbdy	Psme2	Slc3a2	
Bdnf	Dbndd2	Gap43	Ndrg4	Rexo2	Snap25	
Bin1	Dctn6	Gnas	Ngrn	Rpl13a	Tpm1	
Caly	Dtnbp1	Hsd11b1	Nkain4	Rpl5	Tsc2d3	
					U2af1	

## Snap25 DTU across CBS regions

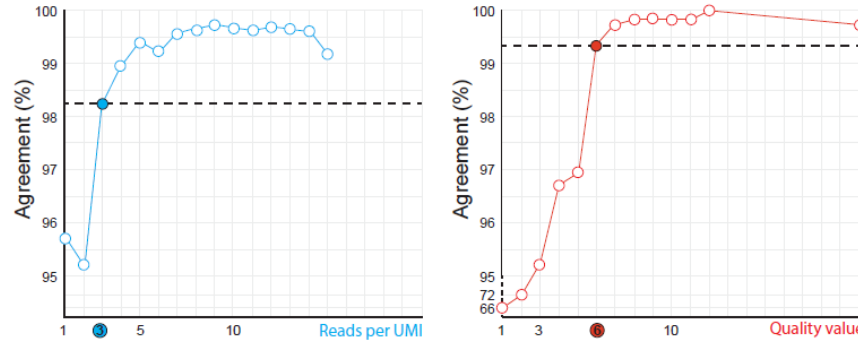
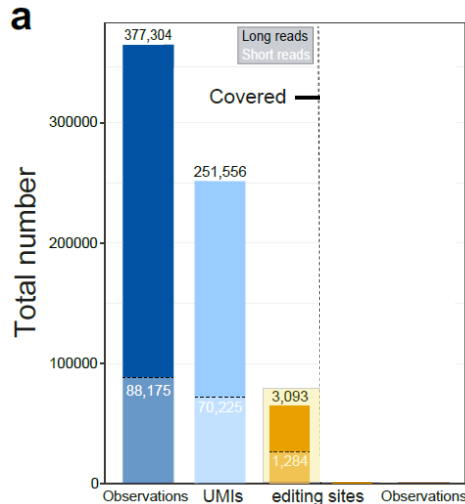
Presynaptic plasma membrane protein involved in the regulation of neurotransmitter release



# SiT reveals full-length sequence heterogeneity (CBS)

High confidence (>99%) SNV call calibration using short-read

- Exploration of 5,817 A-to-I RNA editing sites described in the literature (Ramaswami et al., 2013 (RADAR), Licht et al., 2019)
- Long read high confidence call thresholding, looking at agreement between long and short read base calls for 88,175 shared UMIs
  - number of reads per UMI  $\geq 3$
  - consensus Phred score QV  $\geq 6$

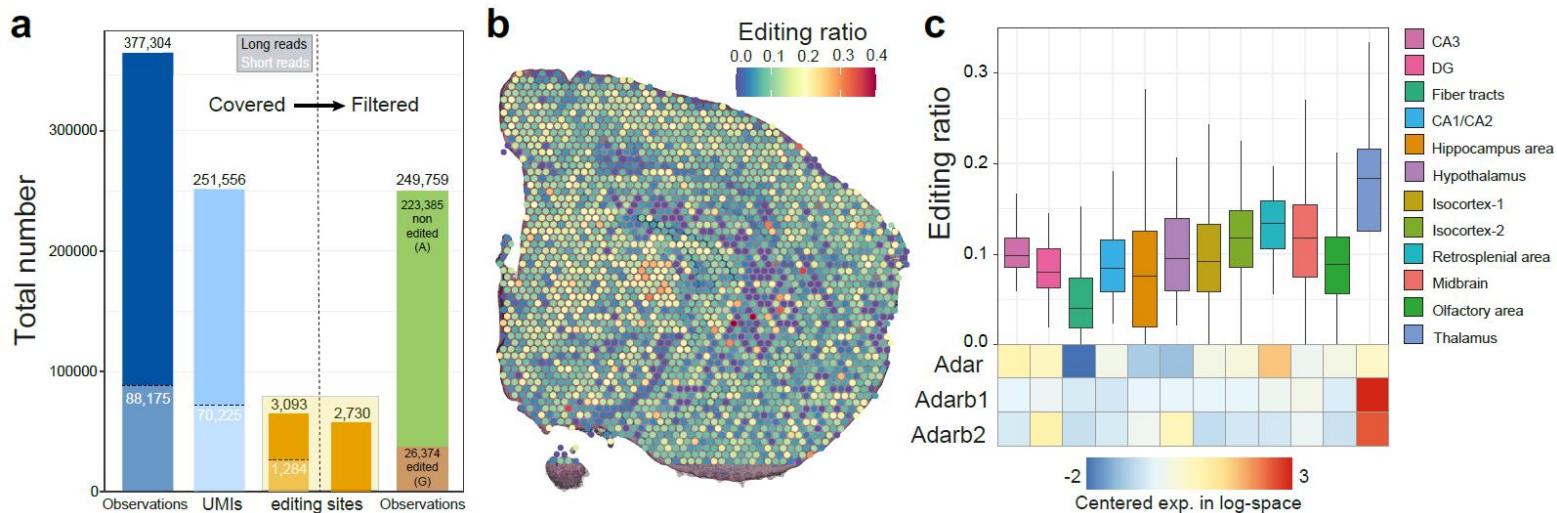


**Supplementary Figure 11. Agreement of editing rates between long-read and short-read data for the genomic regions that are detected by both approaches.** The percentage of agreement between the two sequencing approaches is plotted as a function of nanopore read numbers per UMI (left plot) and nanopore consensus base quality value (right plot). The highlighted thresholds were used for editing site calling with nanopore reads.

# SiT reveals full-length sequence heterogeneity (CBS)

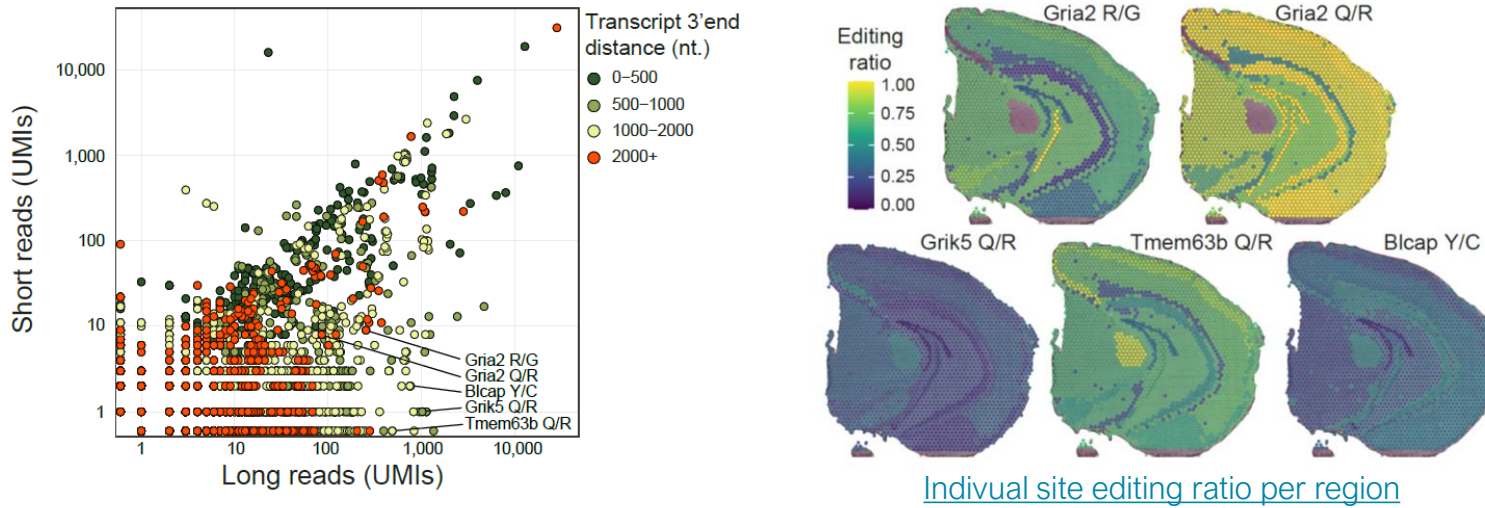
Global A-to-I RNA editing spatial map

- Exploration of 5,817 A-to-I RNA editing sites described in the literature (Ramaswami et al., 2013 (RADAR), Licht et al., 2019)
- Long read high confidence call thresholding, looking at agreement between long and short read base calls for 88,175 shared UMIs
  - number of reads per UMI  $\geq 3$
  - consensus Phred score QV  $\geq 6$



# SiT reveals A-to-I RNA editing specificity in the mouse brain

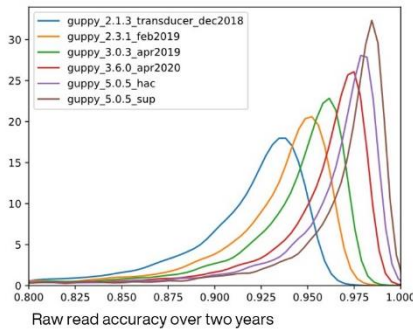
Short vs Long -read editing site calls



# Single cell and Spatial isoform transcriptomics

## Summary

- Accurate single-cell and spatial transcriptomics using Nanopore long-read sequencing is feasible
- Long reads sequencing reveals transcript diversity that is missed with standard short reads workflows
- Single Nucleotide Variation calls (SNV, editing) in single-cell and in a spatial context can be achieved
- **Sicelore-2.1** : we don't need short reads anymore



Nanopore PromethION sequencing

2018: 20M reads/FC, 92% raw read accuracy

2022: 150M reads/FC, 98% raw read accuracy



<https://github.com/ucagenomix/sicelore-2.1>

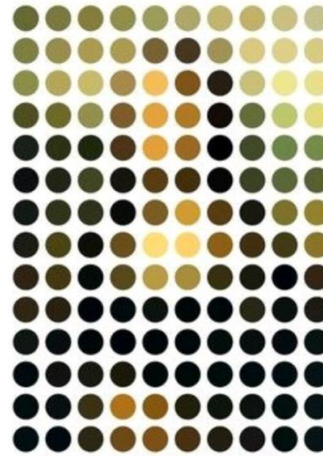
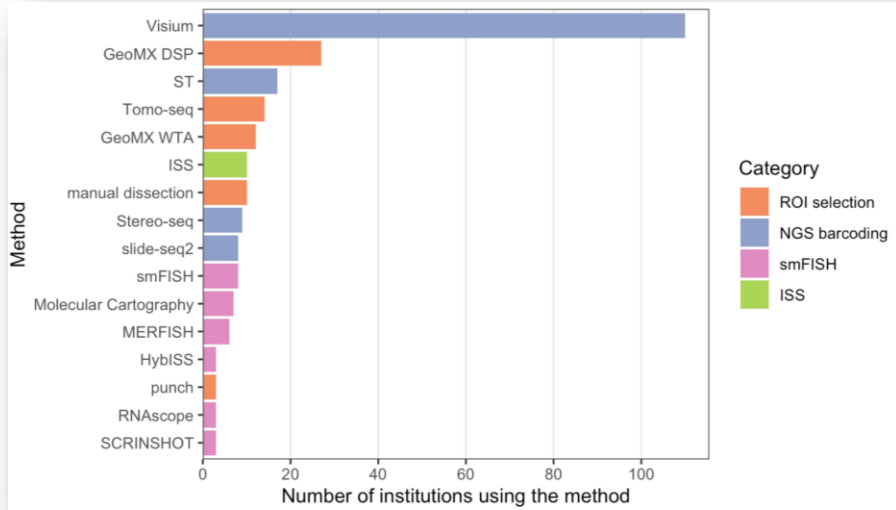
- Visium and single-cell 3' and 5' libraries
- Illumina-free profiling available

# 04

## Spatial single-cell imaging-based transcriptomics

# Spatial transcriptomics technologies (2019-2022)

Visium is widely adopted by academics



But is not the ideal readout for spatial biology  
(Akoya credit rough caricature)

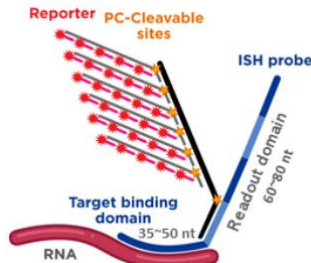
# Spatial imaging technologies (2023)

No more sequencing for direct single-cell resolution



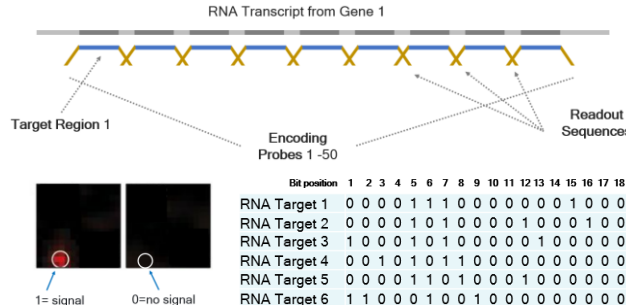
**Nanostring CosMX**  
ISH-based

- 960 targets
- Sensitivity : < 30-80%
- Resolution: 200 nm
- Imaging area: 16 mm<sup>2</sup>



**Vizgen Merscope**  
Merfish

- 500 targets (1,000 soon)
- Sensitivity : 30-80%
- Resolution: 100 nm
- Imaging area: 100 mm<sup>2</sup>



**10xGenomics Xenium**  
Cartana ISS, padlock probes / RCA

- 400 targets
- Sensitivity : 5-30%
- Resolution: 200 nm
- Imaging area: 25 mm<sup>2</sup>



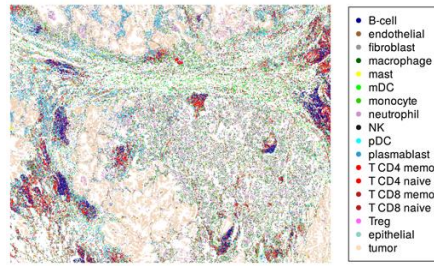
# Spatial imaging technologies comparison

Compare available datasets

## Vizgen Merscope

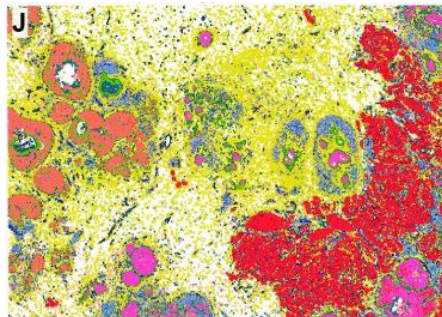
- Xiaowei Zhuang's lab merfish publications
  - Chen et al., Science (2015)
  - Moffitt et al., PNAS (2016), Science (2018)
  - Emanuel G et al., Nature Methods (2017)
  - Xia C. et al., PNAS (2019), Scientific Reports (2019)
  - Zhang M. et al., Nature (2021)
  - ...
- Internal data release program
  - Human Immuno-oncology (**breast**, colon, **lung**, liver, skin, prostate, uterine and ovarian) 500 genes, >4 billion transcripts, 9 million cells
  - Mouse Liver Map (347genes)
  - Mouse brain Receptor Map (483 genes)
- External labs publications
  - Dixon E. et al., Kidney Int. (2022): Kidney
  - Wang et al., Nat. Neuro. (2022): Mouse olfactory Glomerular map
  - Stogsdill et al., Nature (2022): Neocortex microglia
  - ...

## Nanostring CosMx



- Release date: 11/2021
- FFPE Human NSCLC (**Lung**)
- 960 gene targets
- 8 sections for 800k cells
- Imaging area: 8 x 16 mm<sup>2</sup>
- 259,604,214 transcripts
- Mean transcripts/cell: 265

## 10xGenomics Xenium



- Release date: 10/2022
- FFPE Human **Breast** cancer
- 313 gene targets
- 167,885 cells,
- 36,944,521 transcripts
- Imaging area: 40 mm<sup>2</sup>
- Mean transcripts/cell: 193

# Spatial imaging technologies comparison

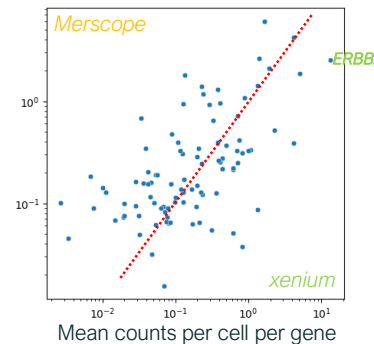
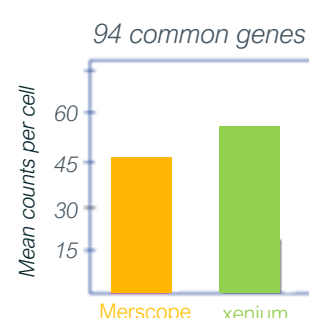
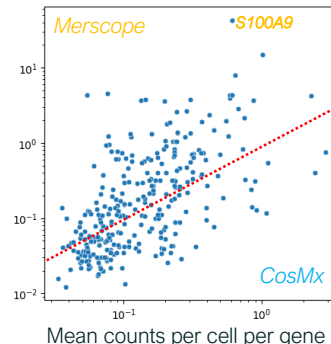
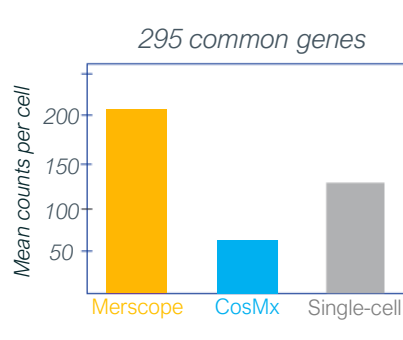
Compare available datasets: Lung and Breast cancer samples



FFPE Human Lung Cancer	Merscope	CosMx
Total cells	353 k (x4)	92 k
Detected transcripts	107 M (x4)	26 M
Gene targets	500	960 (x2)
Total RPKM	9,204	61,680 (x6)
Mean transcripts/cell	302	284



FFPE Human Lung Cancer	Merscope	Xenium
Total cells	713 k (x4)	168 k
Detected transcripts	353 M (x10)	32 M
Gene targets	500	313
Total RPKM	9,909	7,912
Mean transcripts/cell	495	193

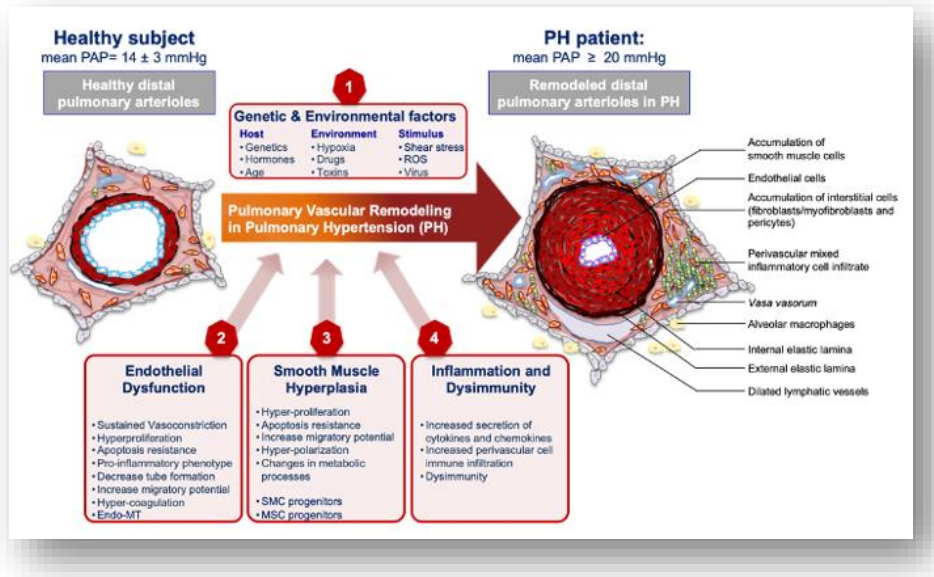


<https://vizgen.com/wp-content/uploads/2022/12/Vizgen-Spatial-Genomics-Data-Quality-eBook-1.pdf>

# PAH : Pulmonary Arterial Hypertension

A rare vascular disorder

Characterized by the presence of occluded pulmonary arterioles resulting from the proliferation of pulmonary artery endothelial cells (PAECs), pulmonary artery smooth muscle cells (PASMCs) and fibroblasts, which leads to right heart hypertrophy and eventual cardiac failure

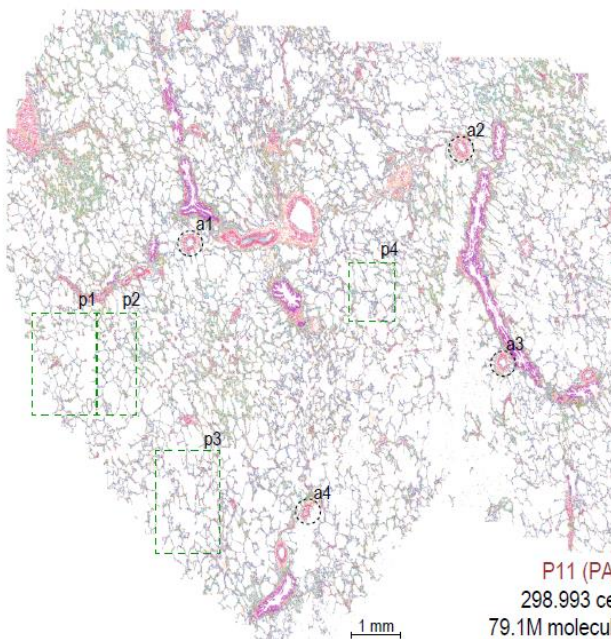
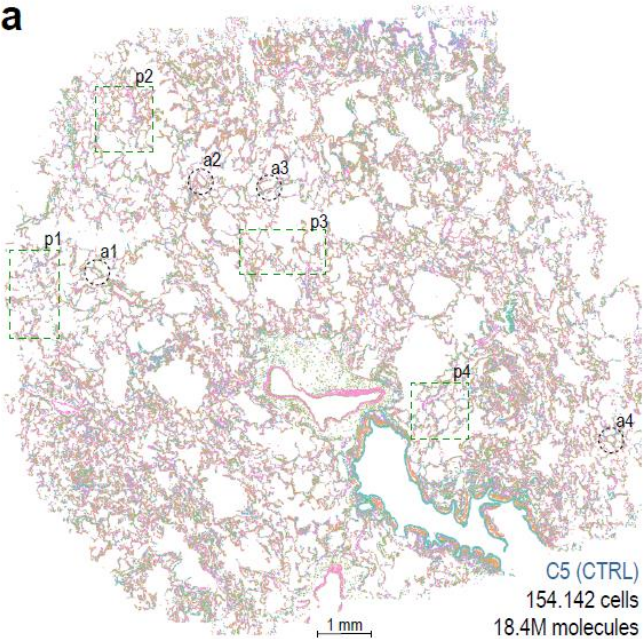


- Defined by a mean pulmonary arterial pressure >20 mmHg
- More frequent in women to men (2:1 to 4:1)
- Different origins:
  - IPAH (idiopathic or sporadic cases),
  - HPAH (heritable case family history) 6-10% monogenic autosomal-dominant - 14% ♂, 42% ♀
  - APAH (associated forms), anorexigens / liver / congenital heart / connective tissue disease

# PAH : Pulmonary Arterial Hypertension

A rare vascular disorder

a

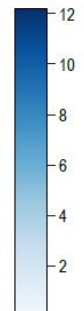


b

C5 P11

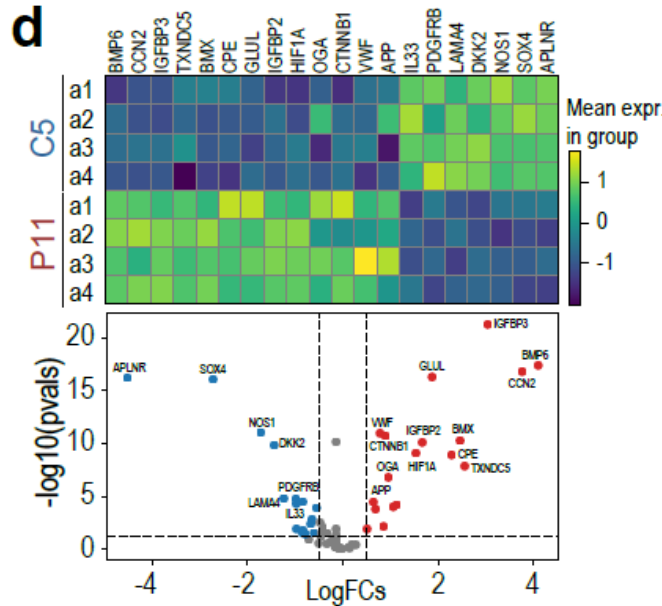
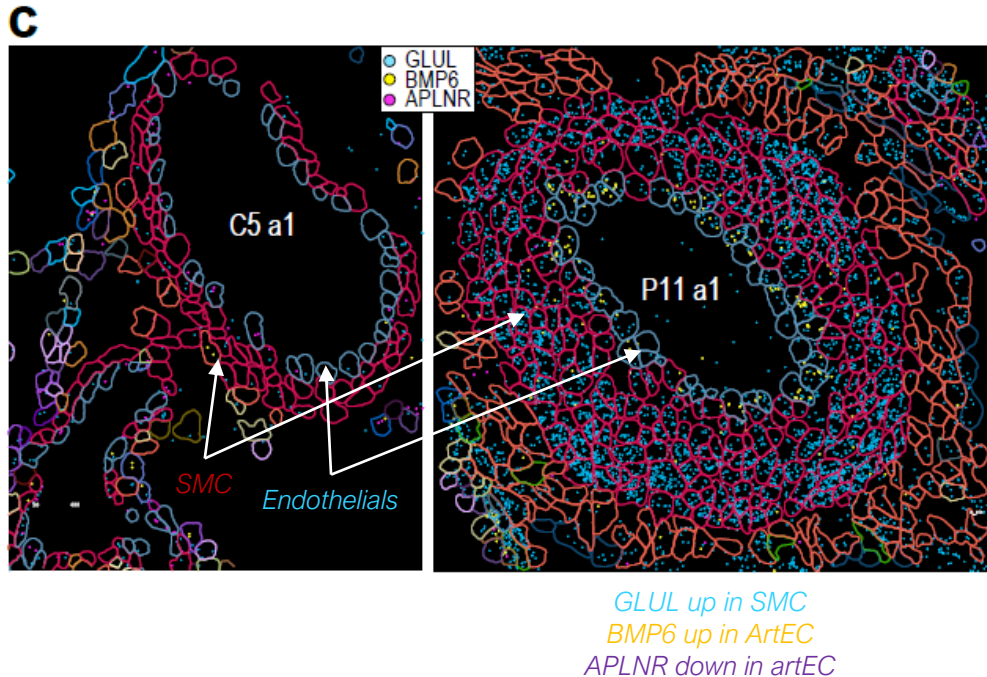
	C5	P11
ArtEC	6.8	3
VeinEC	12	8.8
aCAP	5.2	6.3
gCAP		
Peri		
MyoFibro		
AdvFibro		
AlvFibro		
SMC		
Lymph		
AT0	6.6	9.7
AT1	5.3	6.4
AT2	5.7	3.7
Basal	5.5	4.5
MCC	7.4	10
Secretory		
Plasma		
B	7	1.5
NK		
CD4		
CD8		
DC		
Mono		
Mast		
Megak		
Macrophage	2.3	5.7
Inter-Macro	1.4	5.8

cell type prop.



# PAH : Pulmonary Arterial Hypertension

A rare vascular disorder



# Acknowledgments

Institut de Pharmacologie Moléculaire et Cellulaire



Pascal Barbuy's Lab (IPMC, CNRS, France)

- Rainer Waldmann
- Virginie Magnone
- Marie-Jeanne Arguel
- Yvon Mbouamboua

Joakim Lundeberg's Lab (KTH Royal Institute of Technology, Sweden)

- Joseph Bergenstråhle
- Kim Thrane

Inserm U999 (Le Plessis Robinson)

- Christophe Guignabert
- Ly Tu

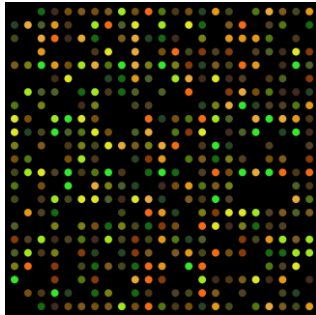


# 05

## Supplementary

# 20 years of transcriptomics

Driven by microfluidics technological developments

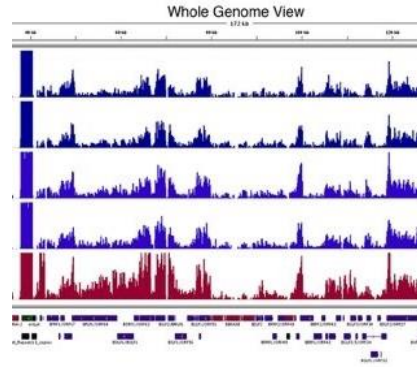


## Early 2000's: DNA microarray

- Large-scale transcriptome
- Oligonucleotide probe tilling
- Fluorochrome signal analysis
- Bulk resolution



Cost : 4k€  
20 samples  
25k genes  
**0.5M matrix**

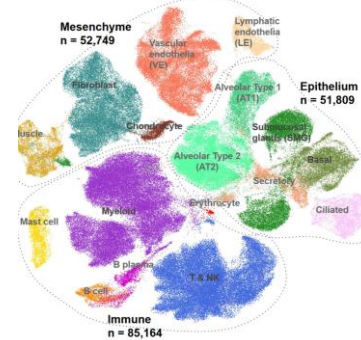


## Late 2000's: RNA sequencing

- Whole transcriptome
- Next Generation Sequencing
- Full-transcript coverage
- Bulk resolution



Cost : 4k€  
20 samples  
50k genes  
**1M matrix**

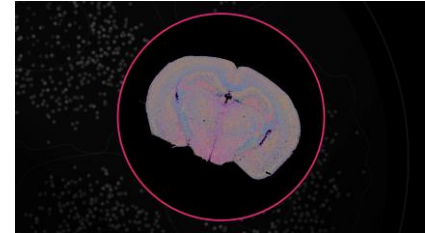


## Mid 2010's: Single-cell

- Whole transcriptome
- Microfluidics + NGS
- 3p-end gene signal (UMI)
- Sensitivity (6%)
- Single-cell / state resolution



Cost : 4k€  
5k cells  
50k genes  
**250M matrix**



## 2020's : Spatial

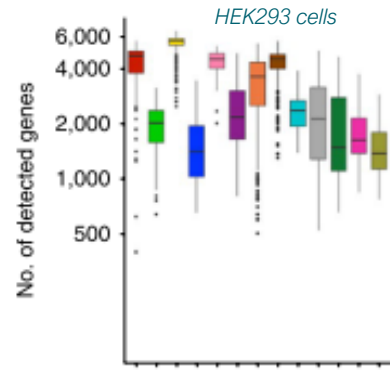
- 500-1000 gene targets
- Imaging analysis
- Multiplexing FiSH (single molecule)
- Sensitivity (30-80%)
- Sub-cellular resolution



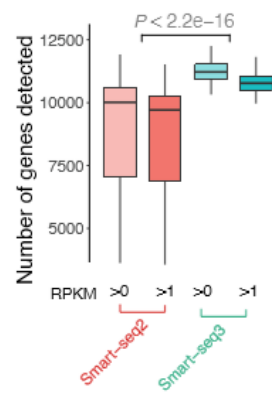
Cost : 4k€  
250k cells  
1k genes  
**250M matrix + Spatial dimension**

# Increase access to in-depth cell transcriptome

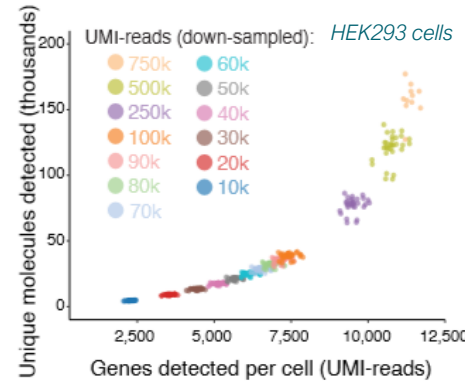
Single cell capture efficiency



Benchmarking single-cell RNA-sequencing  
protocols for cell atlas projects  
Mereu et al., Nat.Biotech, 2020



Single-cell RNA counting at allele- and isoform-resolution using  
Smart-seq3  
Hagemann-Jensen et al., Nature Biotech, 2020



UMIs detected in HEK293 cells

Droplets 10x: 30k

Plate-based : 60k

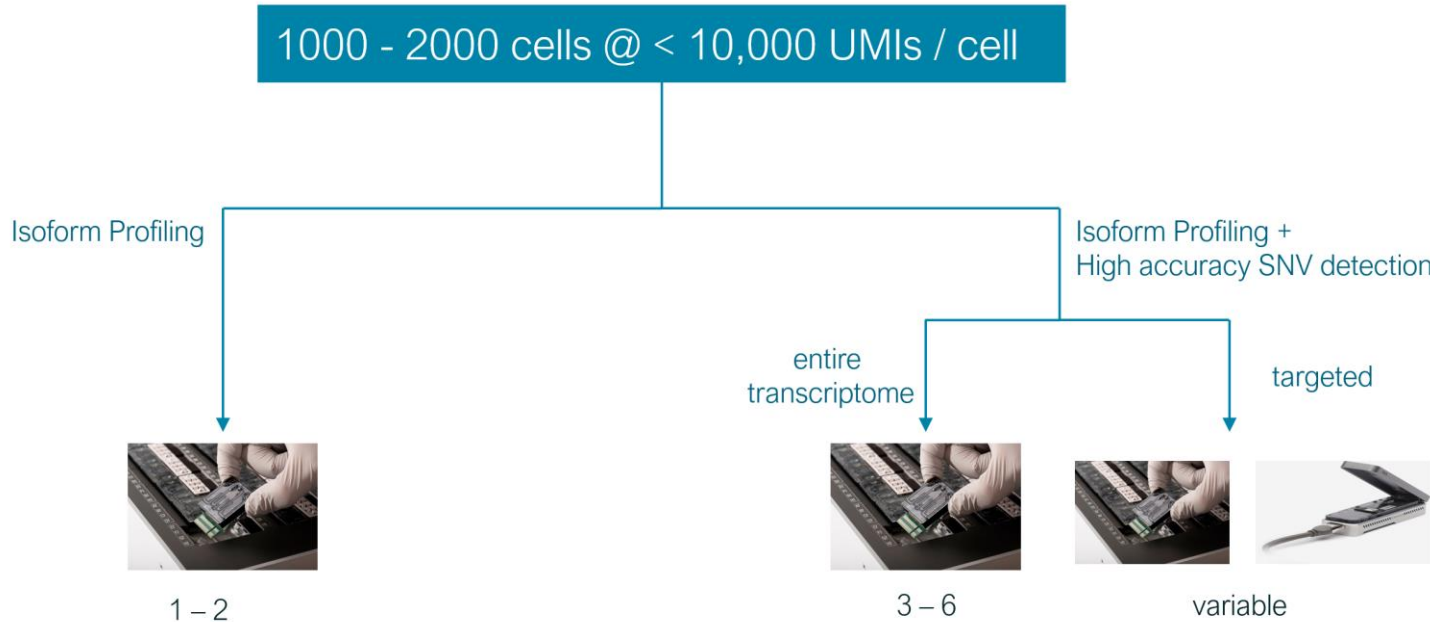
Smart-seq3: 150k



Mantis Microdispenser  
(Formulatrix)

# How many long reads do we need ?

- Depends on number of cells and mRNA content of cells (complexity)



# Full-length Transcriptomics at single cell and spatial resolution

Adding layers of information

---

## Access alternative splicing events

- Huge better characterization of cell transcriptome,
- A potentially crucial layer of understanding for cell type classification,
- Perturb-seq on transcription factor and splicing factor to gain insight into this complex mechanisms

## Access full-length sequence heterogeneity

- A-to-I RNA editing mechanism in-depth description,
- Abnormal cell behavior: cancer cell, access to fusion transcript, access to SNVs to better characterized dysregulated program,
- Clonality tumor exploration, drug resistance experiments,
- Allele-Specific Expression (ASE), imprinting genes landscape exploration (Slide-seq v2, 10µm)

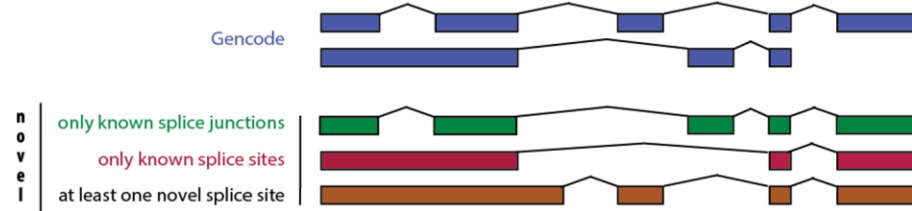
Allele-Specific Transcript Structure (ASTS) to study  
the effects of genetic variants on the transcriptome (sQTL).  
NCM2019, Dafni Glinos, Lappalainen lab , NYGC



now @single cell and spatial resolution

# Novel isoforms detection

E18 mouse brain single cells

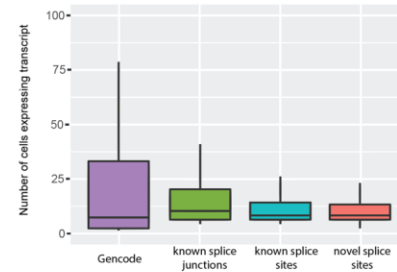


	Total	All splice junction in Illumina data	CAGE peak	polyA site	Final	% of tot
Known Gencode	33,002	33,002	20,533	14,908	11,186	34%
Novel	10,681	8,134	9,164	6,858	4,388	41%
Only known junctions	3,063	3,063	2,644	1,939	1,696	55%
Only known splice sites	2,111	1,905	1,906	1,366	1,115	53%
At least one novel splice site	5,507	3,166	4,614	3,553	1,577	29%

Novel isoforms are expressed at low level

3795 Gencode UMI<sub>s</sub>/cell  
60 novel isoform UMI<sub>s</sub>/cell

Novel isoforms are expressed in fewer cells

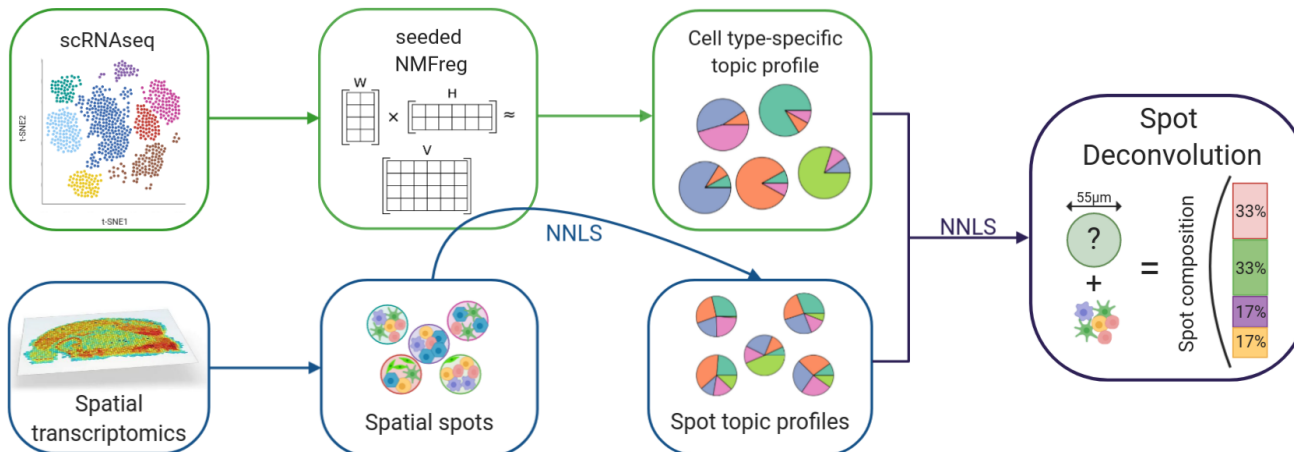


Leakiness of the splicing machinery or physiologically relevant ?

# Spatial spot deconvolution

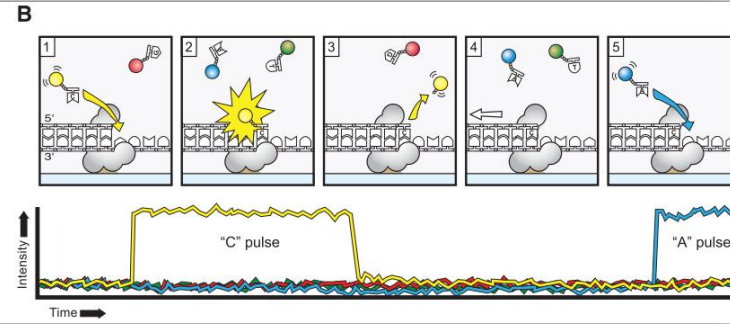
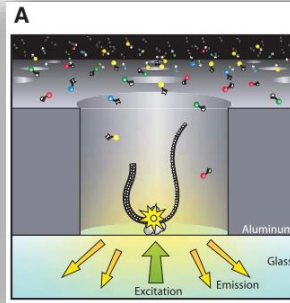
## SPOTlight

- Enables the deconvolution of cell types and cell type proportions present within each capture locations comprising mixtures of cells.
- Is based on finding topic profile signatures to identify the cell type proportions combination fits best the spot to deconvolute.
- Is centered around a seeded non-negative matrix factorization (NMF) regression, initialized using cell-type marker genes, and non-negative least squares (NNLS) to subsequently deconvolute ST capture locations (spots).



# Pacific Biosciences

## Single Molecule Real Time (SMRT) sequencing



(A) DNA template-DNA polymerase complex immobilized at the bottom of each optical nanostructures Zero Mode Waveguide (ZMW) illuminated by laser light from the bottom.

(B) Schematic representation of the phospholinked dNTP incorporation cycle and time trace of detected fluorescence intensity from the ZMW.



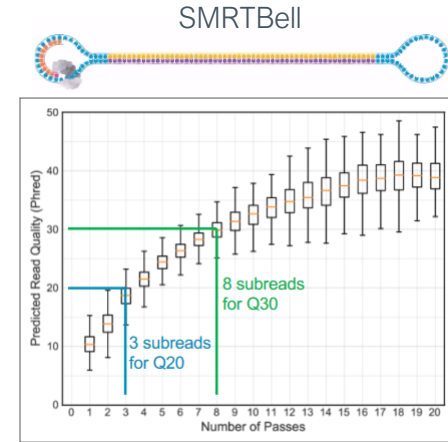
PacBio RS II (Apr.2013)  
• \$750,000  
• 150,000 ZMWs



Sequel I (Oct.2015)  
• \$350,000  
• 1,000,000 ZMWs



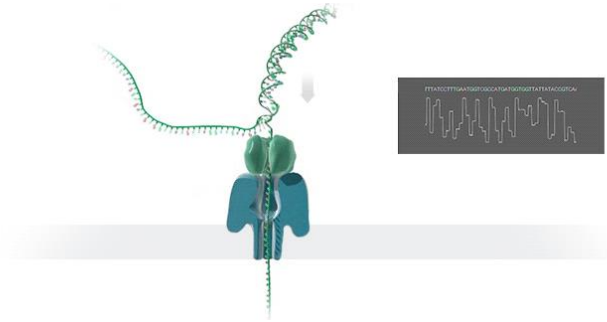
Sequel II (Apr.2019)  
• \$495,000  
• 8,000,000 ZMWs



circular consensus sequencing (CCS)  
> 99.9% accuracy (Q30, 8 passes)

# Oxford Nanopore Technology

## Sequencing through Nanopore



A strand of DNA is passed through a Nanopore. The current is changed as the bases G, A, T or C pass through the pore in different combinations.



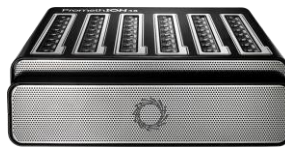
### MinION

- \$1,000
- 512 channels
- Up to 20 Gb / flow cell



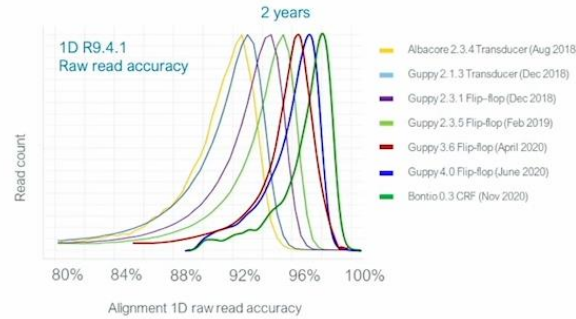
### GridION

- \$50,000
- 5 x 512 channels



### PromethION 24

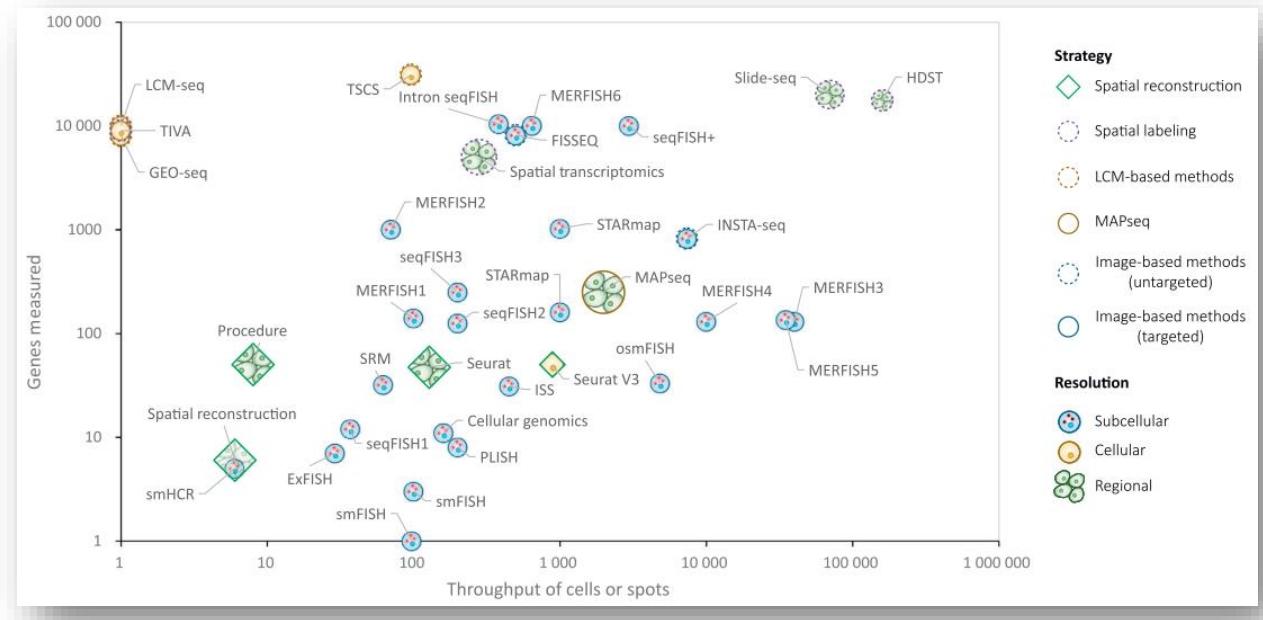
- \$195,000 (120 flow cells included)
- 24 x 3,000 channels
- Up to 120 Gb / flow cell
- 80.000.000 cDNA reads



Nanopore R9.4.1 raw read accuracy improves from 90% to 98% in the last years

# Spatial Transcriptomics approaches

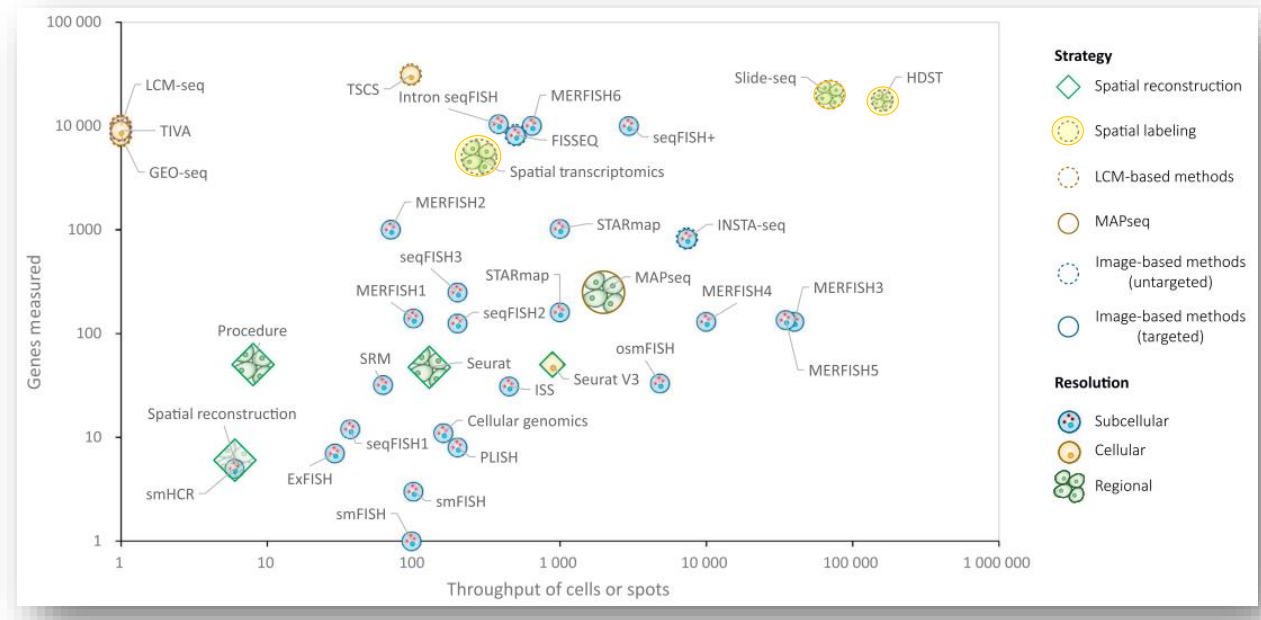
## Throughput of Genes and Cells



Uncovering an Organ's Molecular Architecture at Single-Cell Resolution by Spatially Resolved Transcriptomics  
Liao et al., 2020

# Spatial Transcriptomics approaches

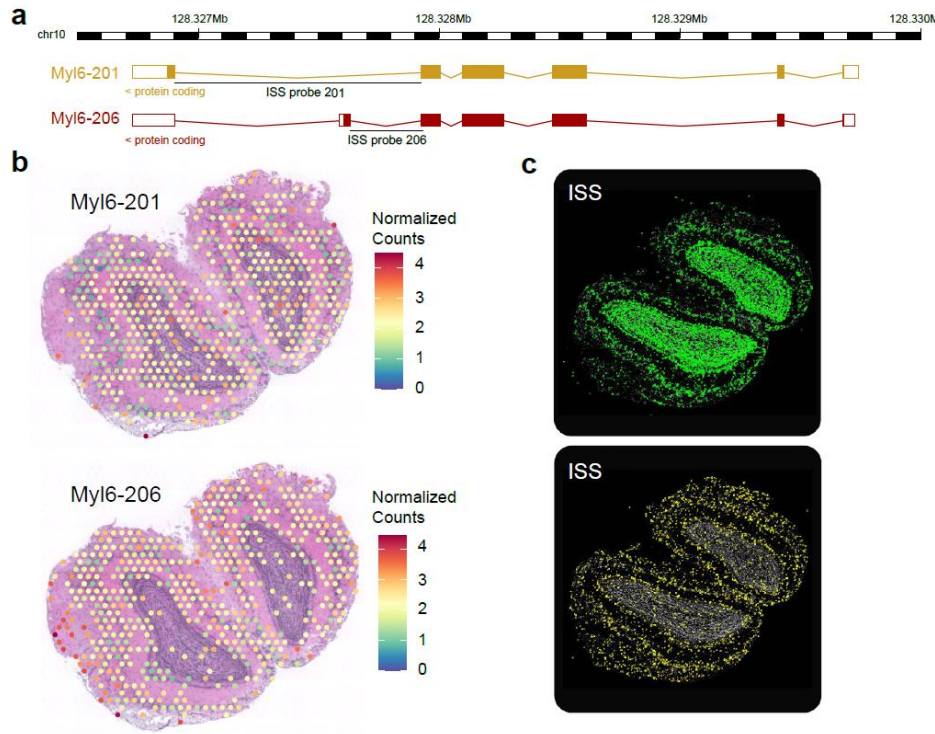
Spatial labelling in-situ then ex-situ sequencing



Uncovering an Organ's Molecular Architecture at Single-Cell Resolution by Spatially Resolved Transcriptomics  
Liao et al., 2020

# SiT reveals specific splicing pattern across regions (OB)

Myl6 Differential Transcript Usage (DTU) across regions (MOB)



Myosin Light Chain 6 (Myl6), codes for the non-phosphorylatable alkali light chain component of the hexameric Myosin motor protein, that has been shown to be involved in neuronal migration and synaptic remodeling in immature and mature neurons

# Increase access to in-depth cell transcriptome

## Spatial resolution

Letter | Published: 07 December 2020

### Highly sensitive spatial transcriptomics at near-cellular resolution with Slide-seqV2

Robert R. Stickels, Evan Murray, Pawan Kumar, Jilong Li, Jamie L. Marshall, Daniela J. Di Bella, Paola Arlotta, Evan Z. Macosko & Fei Chen

Nature Biotechnology (2020) | Cite this article

4105 Accesses | 180 Altmetric | Metrics

- Slide-seqV2 improve library generation, bead synthesis and array indexing to reach an RNA capture efficiency ~50% that of single-cell RNA-seq data (~10-fold greater than Slide-seq), approaching the detection efficiency of droplet-based single-cell RNA-seq techniques.
- In the mouse hippocampus, the capture efficiency of Slide-seqV2 was higher than that of a recently released commercial spatial transcriptomics (ST) technology (**mean UMIs, Slide-seqV2 = 45,772 and 10x Genomics Visium = 27,952** for equal feature size (110 µm diameter binned area)

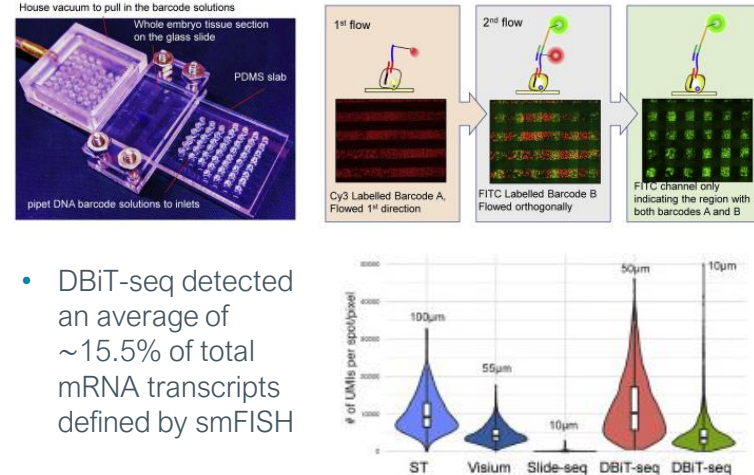
RESOURCE | VOLUME 183, ISSUE 6, P1665-1681.E118, DECEMBER 10, 2020

### High-Spatial-Resolution Multi-Omics Sequencing via Deterministic Barcoding in Tissue

Yang Liu <sup>5</sup> • Mingyu Yang <sup>5</sup> • Yanxiang Deng <sup>5</sup> • ... Yang Xiao • Stephanie Halene • Rong Fan  

Show all authors • Show footnotes

Published: November 13, 2020 • DOI: <https://doi.org/10.1016/j.cell.2020.10.026> • 

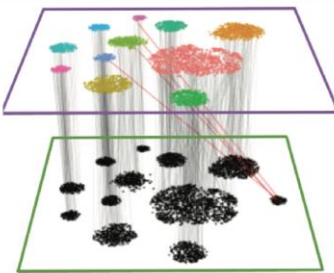


- DBiT-seq detected an average of ~15.5% of total mRNA transcripts defined by smFISH

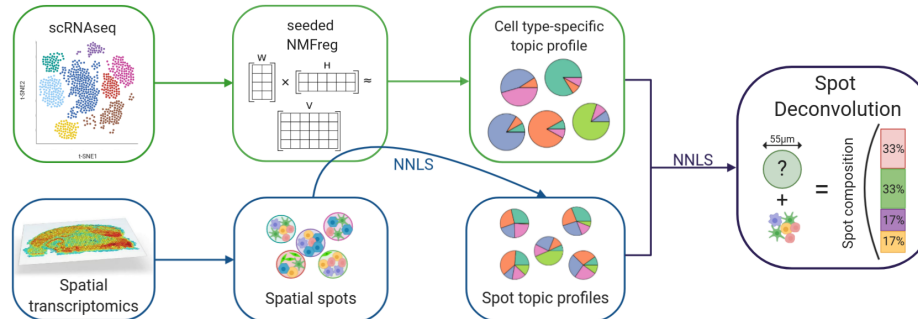
# Spatial spot deconvolution / integration using scRNA-seq

## Seurat integration approach

We consistently found superior performance using integration methods (as opposed to deconvolution methods), likely because of substantially different noise models that characterize spatial and single-cell datasets, and integration methods are specifically designed to be robust to these differences. We therefore apply the 'anchor'-based integration workflow that enables the probabilistic transfer of annotations from a reference to a query set.



**SPOTlight** enables the deconvolution of cell types and cell type proportions present within each capture locations comprising mixtures of cells. **SPOTlight** is based on finding topic profile signatures to identify the cell type proportions combination fits best the spot to deconvolute. SPOTlight is centered around a seeded non-negative matrix factorization (NMF) regression, initialized using cell-type marker genes, and non-negative least squares (NNLS) to subsequently deconvolute ST capture locations (spots).



**Tangram** aligns snRNA-seq data to various spatial data collected from the same brain region, (MERFISH, STARmap, smFISH, and Visium), as well as histological images and public atlases. Tangram can map any type of sc/snRNA-seq data, including multi-modal data such as SHARE-seq data, which we used to reveal spatial patterns of chromatin accessibility. We equipped Tangram with a deep learning computer vision pipeline, which allows for automatic identification of anatomical annotations on histological images of mouse brain.

